Additive Manufacturing of Metals and Alloys

9. Mechanical properties of AM parts

February 2023

Prof. Roland Logé
MER Dr. Christian Leinenbach
Dr. Charlotte de Formanoir

EPFL

Outline

- Thermal gradients and plastic deformation
- Dislocation density and cell structure
- Grain and subgrain size
- Precipitation and chemical segregation
- Texture and anisotropy
- Cyclic loading and fatigue

Thermal gradients and plastic deformation

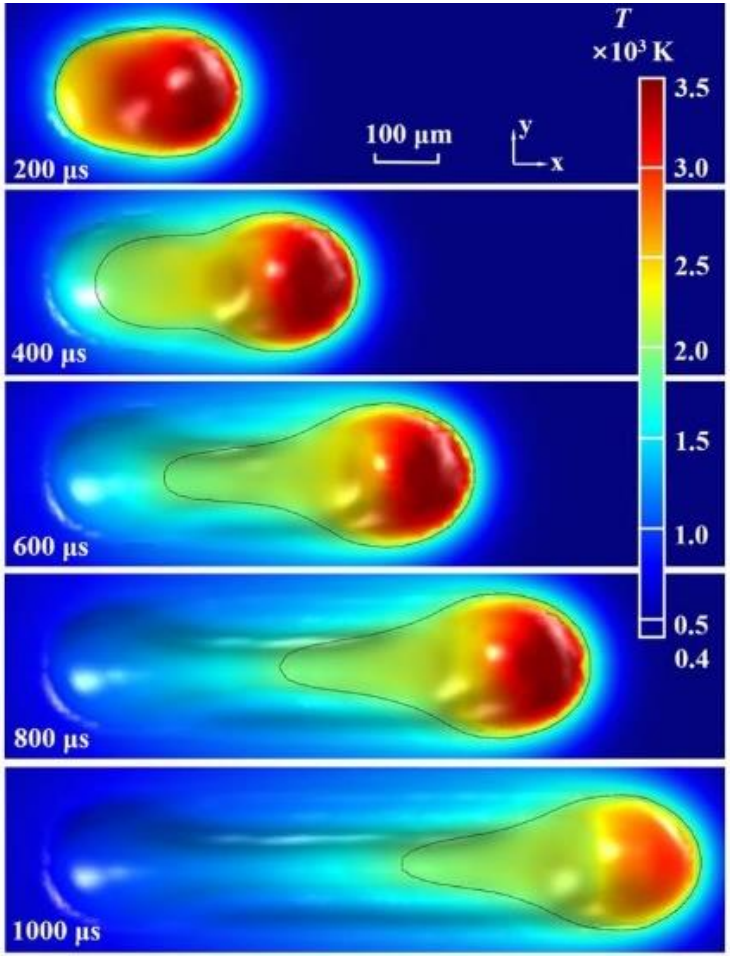

- Very high spatial gradients of T
- Time scale also very short

➡ Neigboring zones undergo different thermal strain / phase transformation

➡ May result in local plastic strain

Plastic strain can accumulate during successive line scans, and lead to significant dislocation density

Measured T profiles in the melt pool (Ti-64)

T

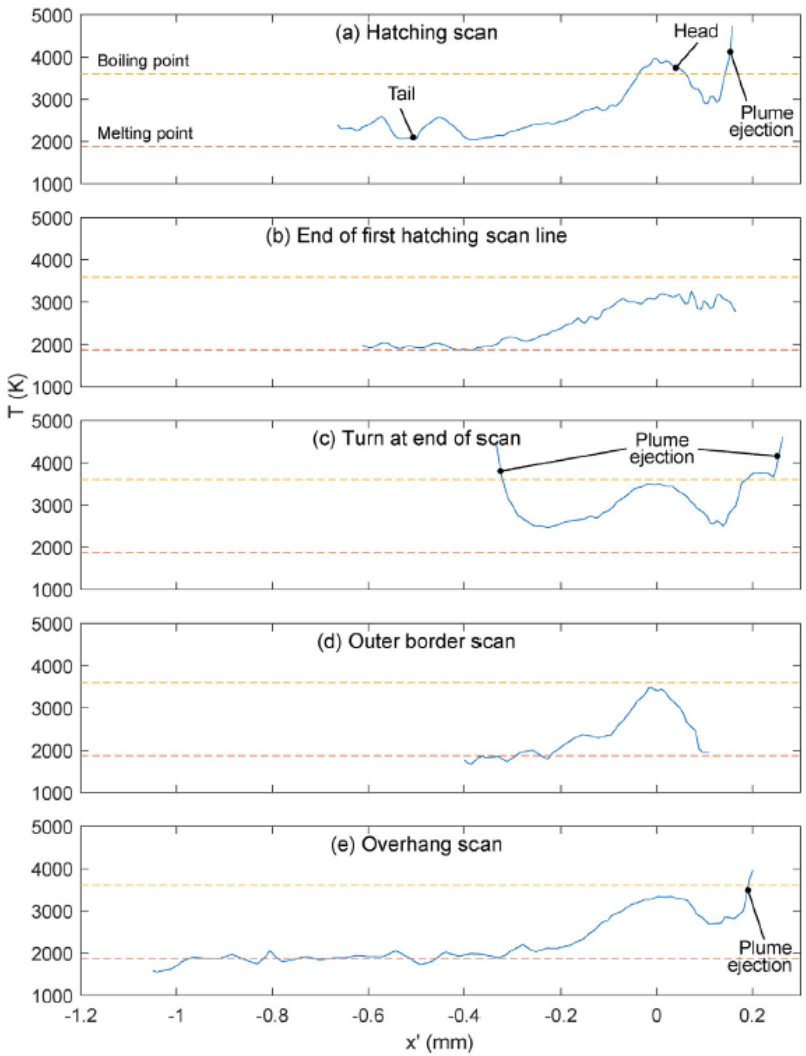

Distance to the center of the laser beam

- Temperature vs distance profiles, Ti-64
- Through a centre line from the head of the melt pool to the tail
- Profiles taken near the end of a laser pulse

- **Boiling point** is often reached

- T gradient **varies a lot in melt pool :** solidification microstructure should relate to the T gradient near the solidification T

P.A. Hooper, Melt pool temperature and cooling rates in laser powder bed fusion, Additive Manufacturing 22 (2018) 548–559

Cooling rate and T gradient **in the solid state**

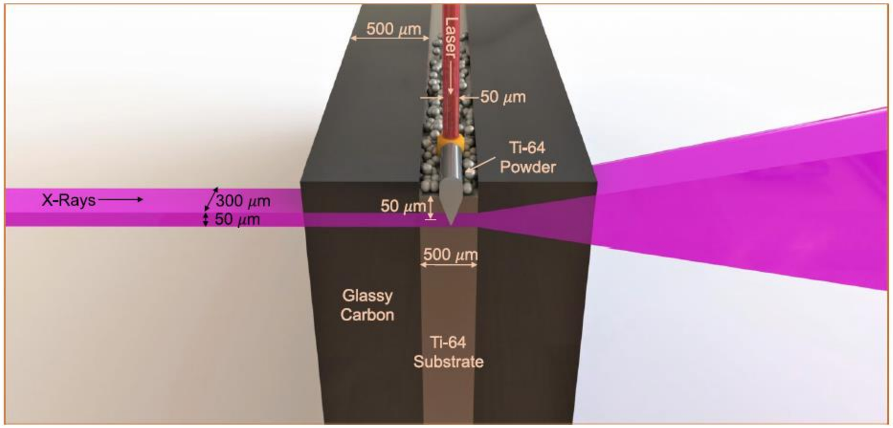

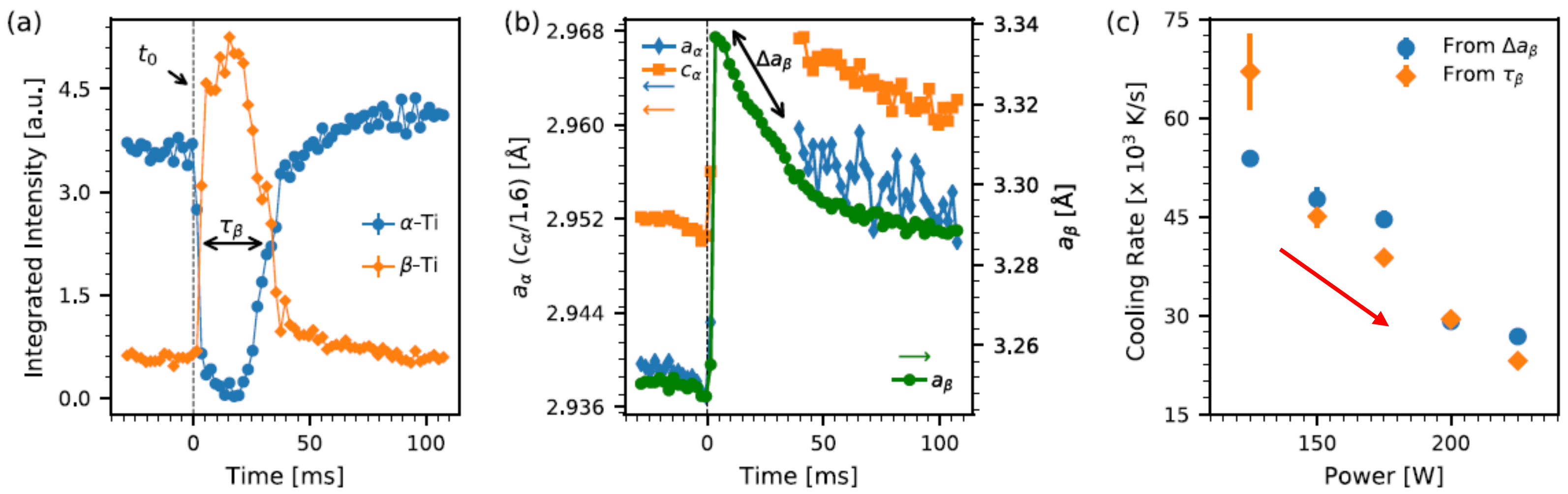

Cooling rate in the high temperature β phase (Ti-64) **decreases with increasing laser power**
→ **Lower** temperature gradients in the solid phase

Thampy, V., Fong, A.Y., Calta, N.P. *et al.* Subsurface Cooling Rates and Microstructural Response during Laser Based Metal Additive Manufacturing. *Sci Rep* **10,** 1981 (2020). https://doi.org/10.1038/s41598-020-58598-z

LPBF processing and stored (dislocation) energy

Normalized enthalpy vs normalized melt pool depth

$$\Delta H = \frac{\alpha_p \boldsymbol{P}}{\sqrt{\pi \omega^3 \boldsymbol{V} D}} \qquad \Delta h = \rho(C_p \Delta T + L_m)$$

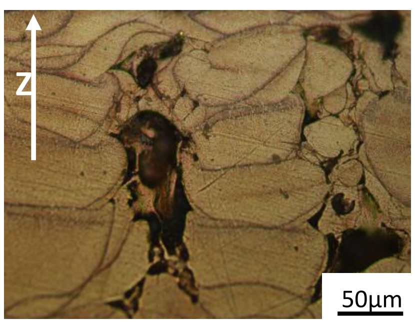

- **Lack of fusion (LoF)**

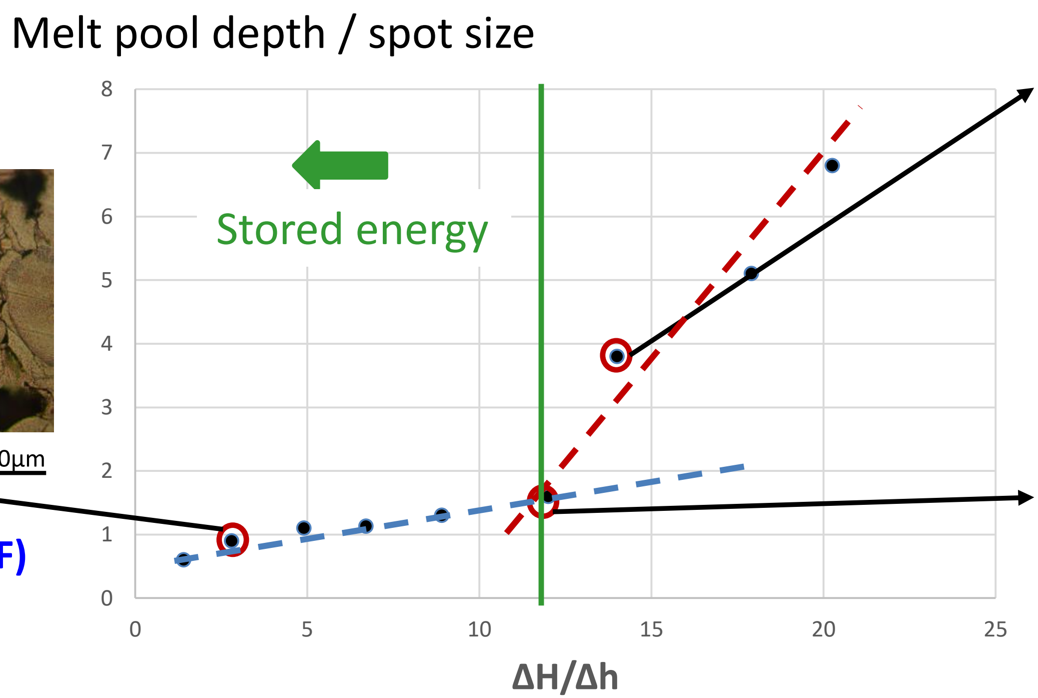

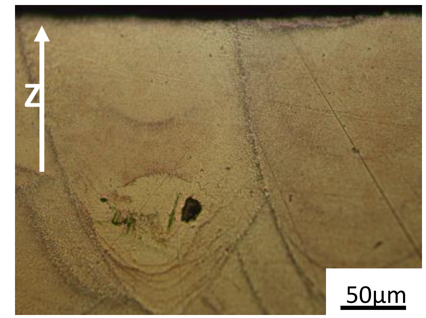

- **Keyhole porosities**
- Deep melt pool

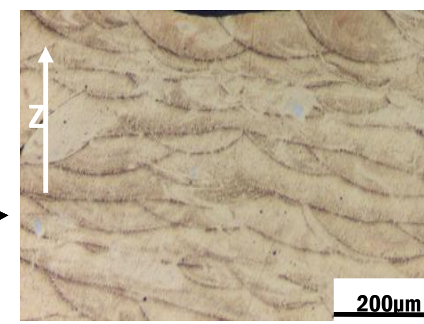

- No Keyhole, No LoF

Conduction mode

Stored energy tends to increase when approaching LoF (reduced amount of heat, large thermal gradients)

Large temperature gradient → geometrically necessary dislocations

Extreme example : rigid (cubic) inclusion embedded in a ductile matrix – plastic deformation

- Dislocations move and interact with inclusions. They bend around them, and need a critical Orowan shear stress to bypass them, given by Gb/d, where d is the mean distance between inclusions, b the Burgers vector, and G the elastic shear modulus.
- Bypassing inclusions leaves behind Orowan dislocation loops.
- These dislocation loops **accommodate the strain incompatibility** between the inclusion and the matrix
- Image forces exist between dislocations and a rigid interface, which maintain the Orowan loops at a certain distance from the inclusions.
- The Orowan loops can minimize their energy by transforming into prismatic, sessile loops.

- Dislocation loops are « **geometrically necessary** ». They increase the hardness of the ductile matrix.

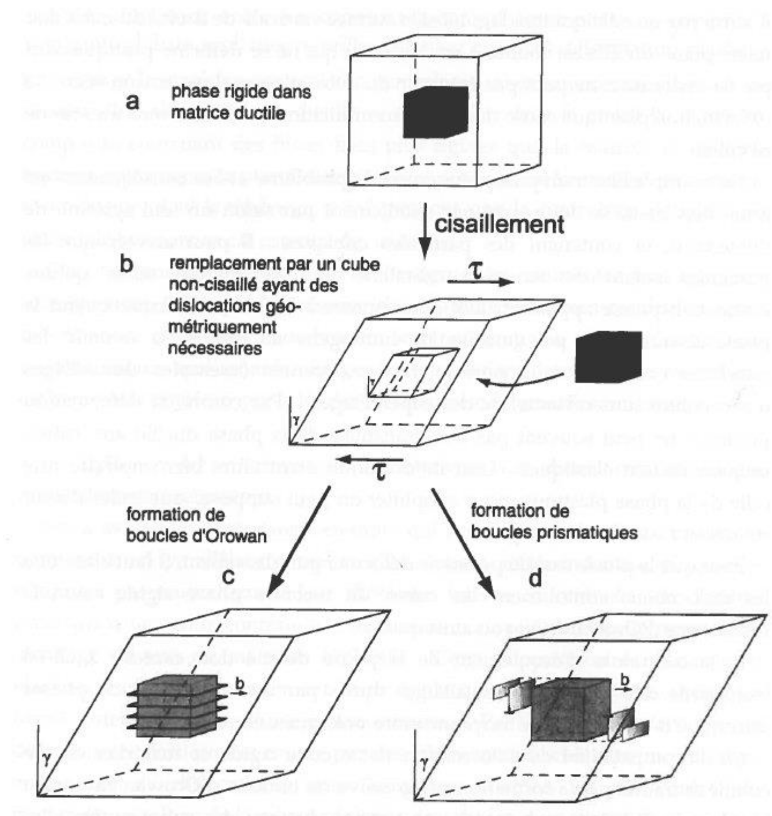

Dislocations géométriquement nécessaires résultant de la présence, au sein d'un cristal déformé par cisaillement selon un système de glissement, d'une inclusion rigide cubique. Les dislocations géométriquement nécessaires peuvent être de plusieurs types, mais expriment toujours le besoin de rétablir la compatibilité entre le cristal déformé et ses frontières.

[Déformation et rupture des matériaux à basse température, tome 1, A. Mortensen & T. Kruml]

Geometrically necessary dislocations

Plastic deformation under large strain gradients

- A crystal is conceptually divided in several neighboring zones.
- Each zone undergoes a different plastic deformation, due to the gradient in the applied load.
- Dislocations of the same type and of opposite sign annihilate.
- The excess of dislocations remaining after annihilation is proportional to the strain gradient in the direction of the Burgers vector.

- In polycrystals, there are large strain gradients near grain boundaries. Geometrically necessary dislocations therefore appear expecially there. They do not move but interact with other dislocations and **increase strain hardening**.

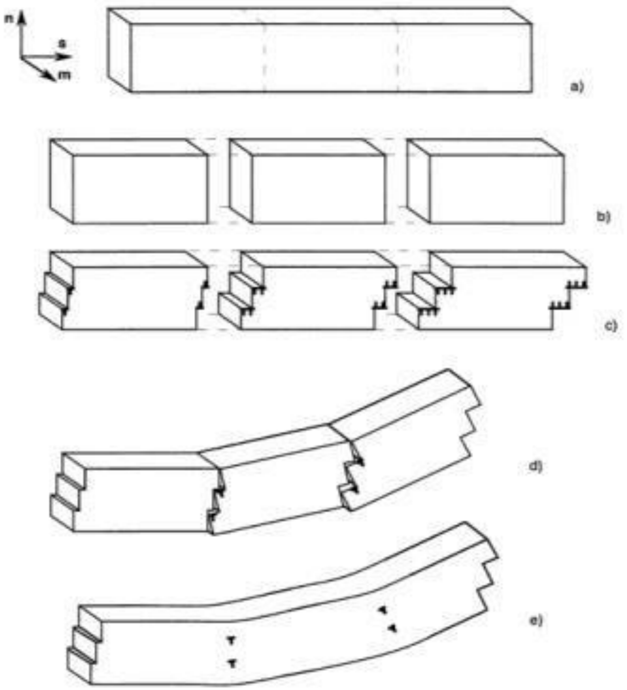

Arsenlis A., Parks D. M., Crystallographic aspects of geometrically-necessary and statistically-stored dislocation density. Acta Materialia, 47, pp. 1597-1611, 1999.

Link between dislocation density ρ and flow stress

ρ m / m³

ρ intersections / m²

$1/\rho$ m² / intersection

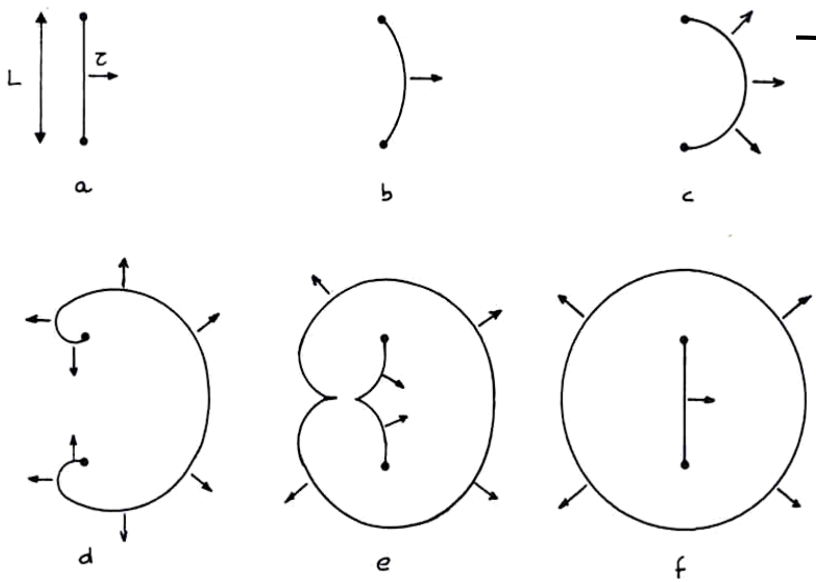

Frank & Read mechanism

$$\tau_c = \beta \frac{Gb}{L}$$

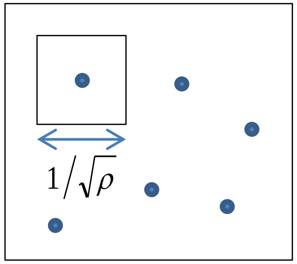

Arbitrary plane

- L is the distance between obstacles created by interaction with other dislocations :

$$L \approx \rho^{-1/2}$$

- Friction forces and other obstacles :

$$\tau = \tau_0$$

$$\tau = \tau_0 + \alpha G b \sqrt{\rho}$$

(α = 0.2..0.3 < β because all dislocations are not obstacles)

Pure FCC metals : $\rho \approx \left(\frac{\tau}{\alpha G b} \right)^2$

Dislocation density and cell structure

Hardening stages in a single crystal

- The hardening rate θ varies as a function of the accumulated strain
- Stage I corresponds to only 1 slip system activated, with the highest Schmid factor
- Stage II activates new slip systems, leading to a strong increase of strain hardening due to dislocation interactions

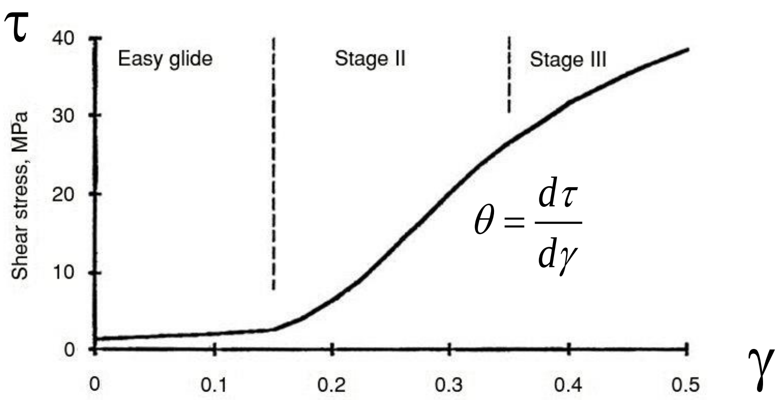

- In stage III, θ decreases with strain
- Stage III features depend on T and strain rate
  - Thermal activation, allowing the reduce / bypass accumulated obstacles to dislocations
  - If T is high, stage III can start almost immediately
  - Cross slip of screw dislocations is activated, especially when the stacking fault energy is high (e.g. Aluminium).

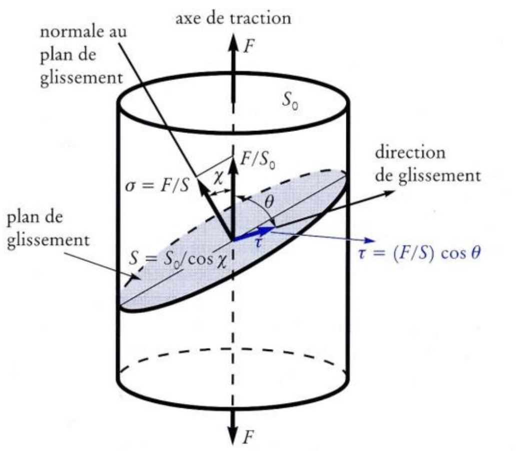

$$\tau = \frac{F}{S_0} \underbrace{\cos\theta \cos\chi}_{m}$$

m = Schmid factor

Hardening stage III

Energy minimization, resulting from attracting forces between dislocations, with dislocation reorganization and annihilation

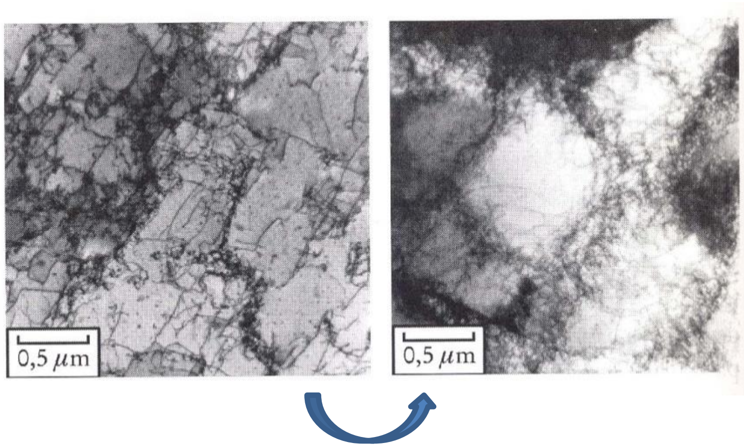

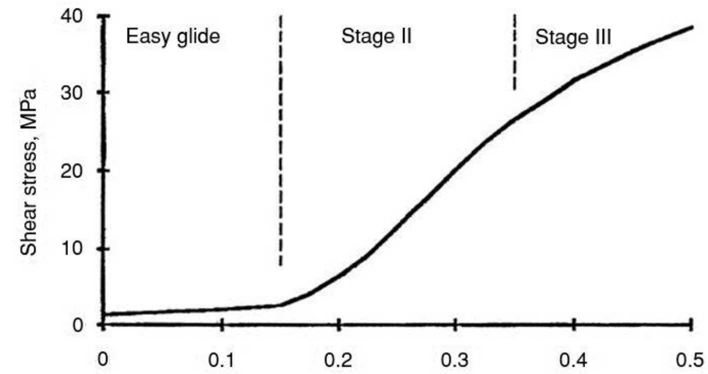

- In stage III, dislocations reorganize themselves into cells and form cell walls.
- This is more effective if dislocations are mobile, with the capability of cross slip and dislocation climb, leading to the structure recovery by energy minimization and dislocation annihilation.

Dislocation density and cell structure in AM

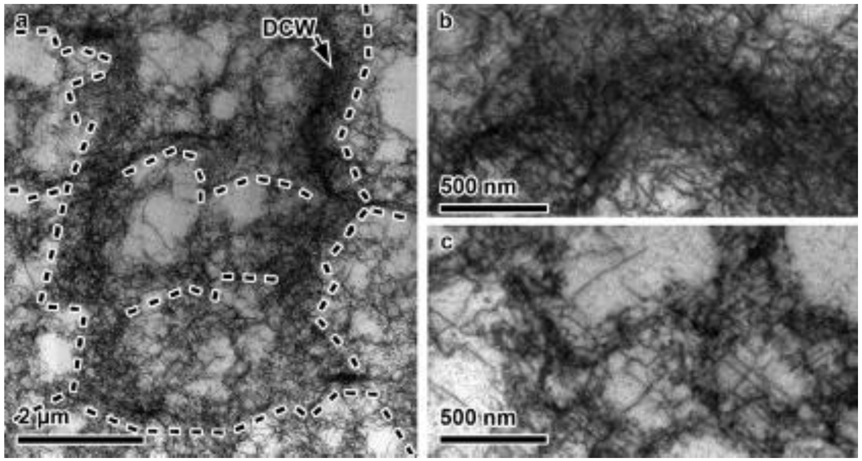

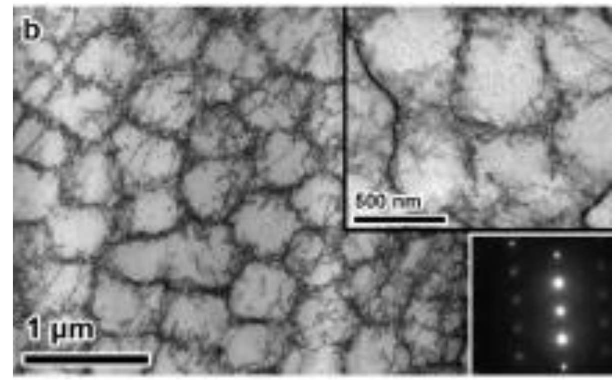

316L stainless steel

K.M. Bertsch et al., Acta Materialia 199 (2020) 19–33

- Dendritic micro-segregation, precipitates, or local misorientations influence how the dislocations organize during processing

- "AM dislocation structures originate from thermal distortions during printing, which are primarily dictated by constraints surrounding the melt pool and thermal cycling."

Grain size and subgrain size

Hall-Petch law

- Grain boundaries are obstacles to the motion of dislocations.
- Arrested dislocations induce a stress on the source of dislocations. If their number *n* is large enough, this stress will oppose enirely to the applied stress τ_a, and the source will stop emitting dislocations when :

$$n = \frac{\pi \alpha D \tau_a}{Gb}$$

(α constant close to 1)

- The stress τ acting on an obstacle by a dislocation pile up under and applied stress τ_a is :

$$\tau = n \tau_a$$

- The yield stress is supposed to be the stress allowing to transmit plastic deformation from one grain to another. For example, by activation of Frank & Read sources on the other side of the grain boundary. The condition is therefore :

$$\tau = n \tau_a \geq \tau_c$$

i.e.

$$\tau_a \geq \sqrt{\frac{Gb\tau_c}{\pi \alpha D}} \propto D^{-1/2}$$

In AM, very fast cooling rates from the melt result in reduced grain size *D* compared to other processes

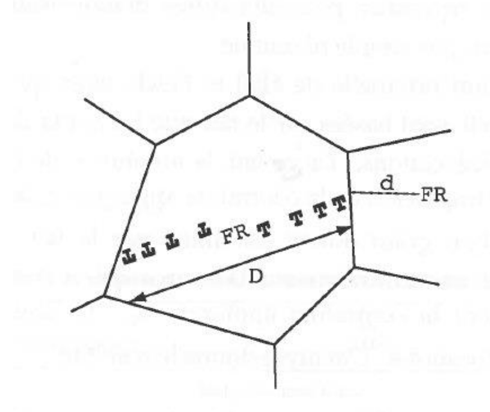

[Déformation et rupture des matériaux à basse température, tome 1, A. Mortensen & T. Kruml]

Grain size and subgrain size

Subgrain structure

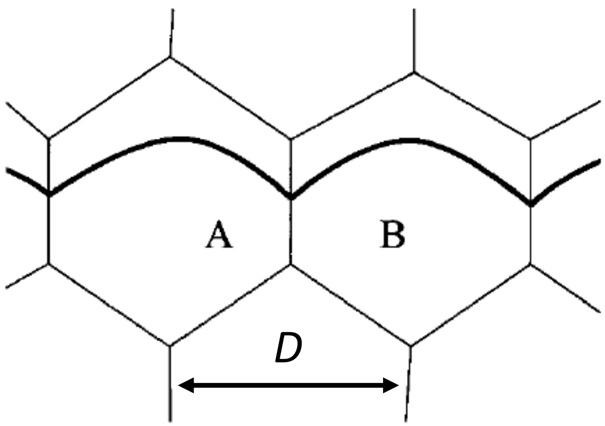

E. Nes, K. Marthinsen & B. Holmedal (2004) The effect of boundary spacing on substructure strengthening, Materials Science and Technology, 20:11, 1377-1382

$$\tau_c = \beta \frac{Gb}{L}$$

L = mean distance between obstacles

- For a grain structure, *L* is the mean distance between dislocations : $L \approx \rho^{-1/2}$
- For a subgrain/cell structure, *L* becomes the mean boundary spacing :

$$\tau \approx \alpha \frac{G\,b}{D}$$

Differs from Hall-Petch !

Precipitation and chemical segregation

- Due to the very high cooling rates operating in AM, precipitates often do not have the time to nucleate or to grow.
- The material is then supersaturated with solute atoms which should have precipitated according to the (equilibrium) phase diagram.

- High cooling rates from the melt also induce chemical segregations

- Depending on the state of precipitation and chemical segregation, hardening mechanisms will operate in the AM material and influence the formation of cell structures.

Example : 316L steel

Cr **micro-segregation** and Fe depletion at large dislocation cell walls

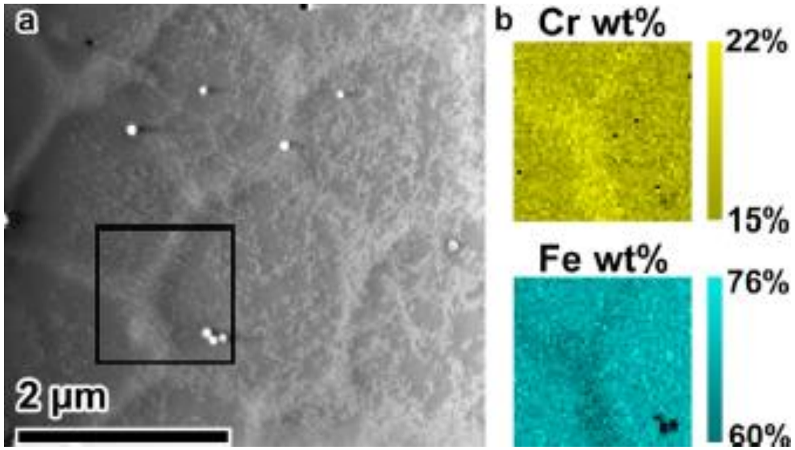

K.M. Bertsch et al., Acta Materialia 199 (2020) 19–33

Precipitation and chemical segregation

Example : 316L steel

P = oxide precipitate
F = ferrite inclusion
D = dislocation

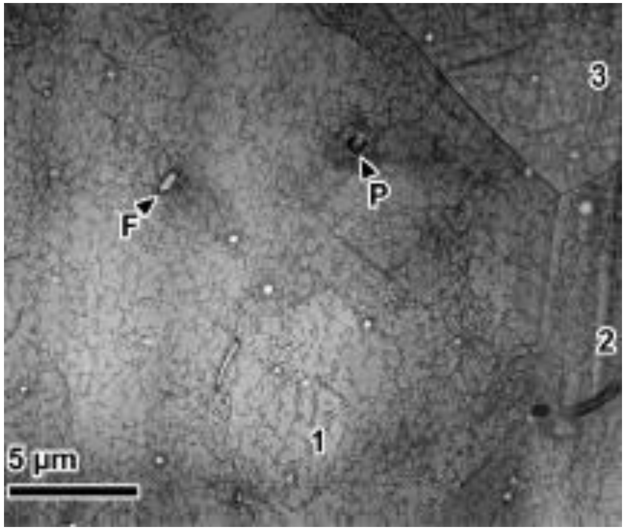

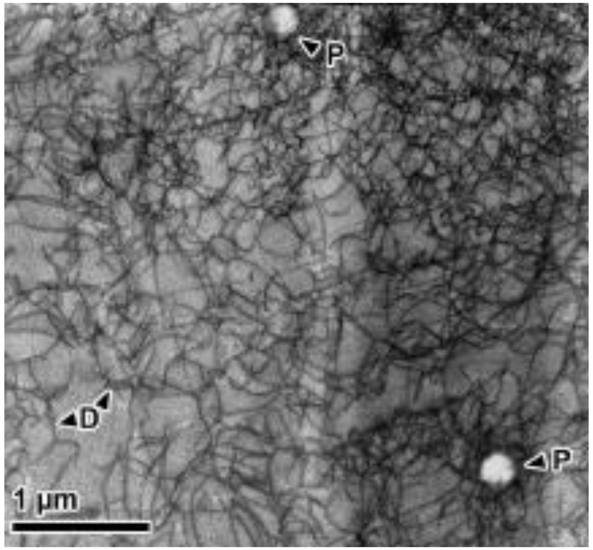

Si, Mn, and Cr oxide fine precipitates approximately 15 nm in diameter on average, primarily in cell walls but also in cell interiors.

K.M. Bertsch et al., Acta Materialia 199 (2020) 19–33

Precipitation strengthening

- In the presence of precipitates, with mean interdistance *d* :
  - The dislocation first curves,

$$\tau = \frac{Gb}{2R}$$

  - The radius of curvature R is minimal when R = *d*/2 :

$$\tau = \tau_c = \frac{Gb}{d}$$

  - Beyond, *R* increases again, and neighboring segments of dislocation annihiliate, leaving a geometrically necessary Orowan loop around each precipitate

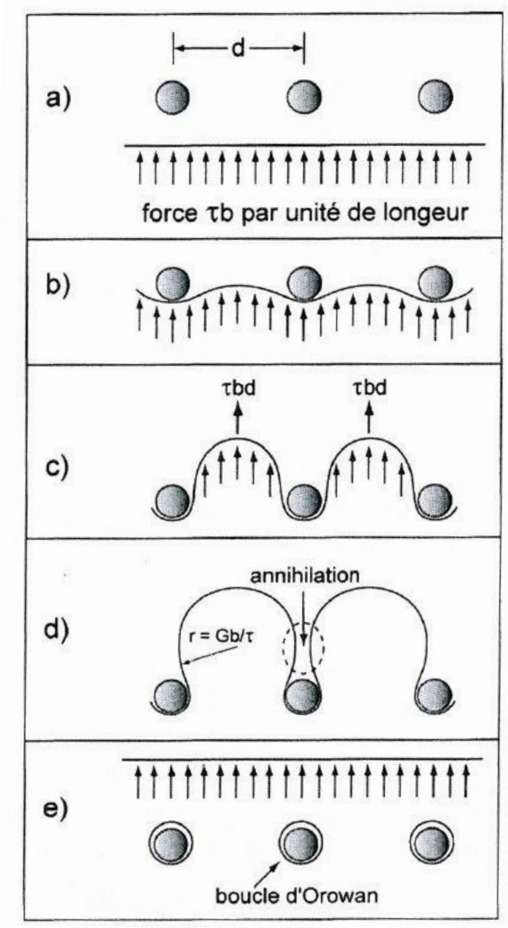

Orowan mechanism

[Déformation et rupture des matériaux à basse température, tome 1, A. Mortensen & Tomas Kruml]

Zener grain boundary pinning

- Second phase particles or precipitates represent pinning forces for the motion of grain boundaries.

- At the junction between grain boundary and particle, the contact angle is $\pi/2$ due to balance of capillary forces.
- Force *F* in the direction of boundary motion:

$$F = 2\pi r \sigma_{jg} \cos\theta \sin\theta = \pi r \sigma_{jg} \sin 2\theta$$

$\sigma_{jg} = \gamma_s$ Grain boundary energy per unit area

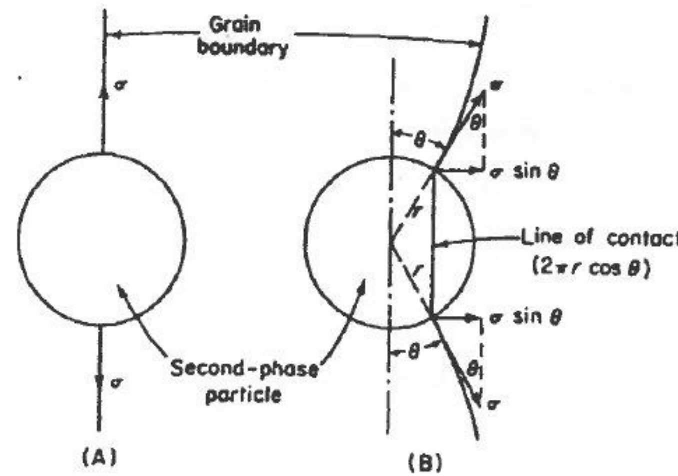

Interation entre un joint de grain et une inclusion sphérique.

[Déformation et rupture des matériaux, Tome 3, A. Mortensen]

Wikipedia, « Zener pinning »

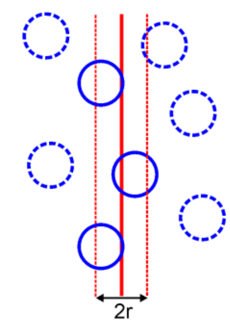

- *F* reaches its maximum for $\theta = \pi/4$.
- Let N be the number of particles per m^3, and assume an overall plane boundary
- The boundary intersects 2*r N* particles per m^2.
- If f is the volume fraction of particles :

$$f = \frac{4}{3}\pi r^3 N$$

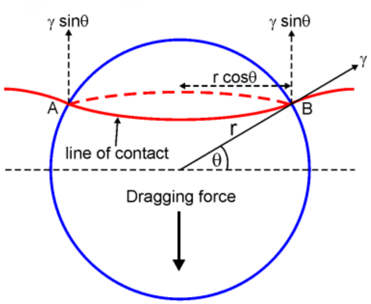

- It results a pinning pressure (assuming *F* = *Fmax* everywhere) :

$$P_Z = F_{\max} 2rN = \frac{3 f \gamma_s}{2r}$$

Zener pressure → At a given *f*, the Zener pressure increases if the particles size (*r*) decreases

Zener pinning

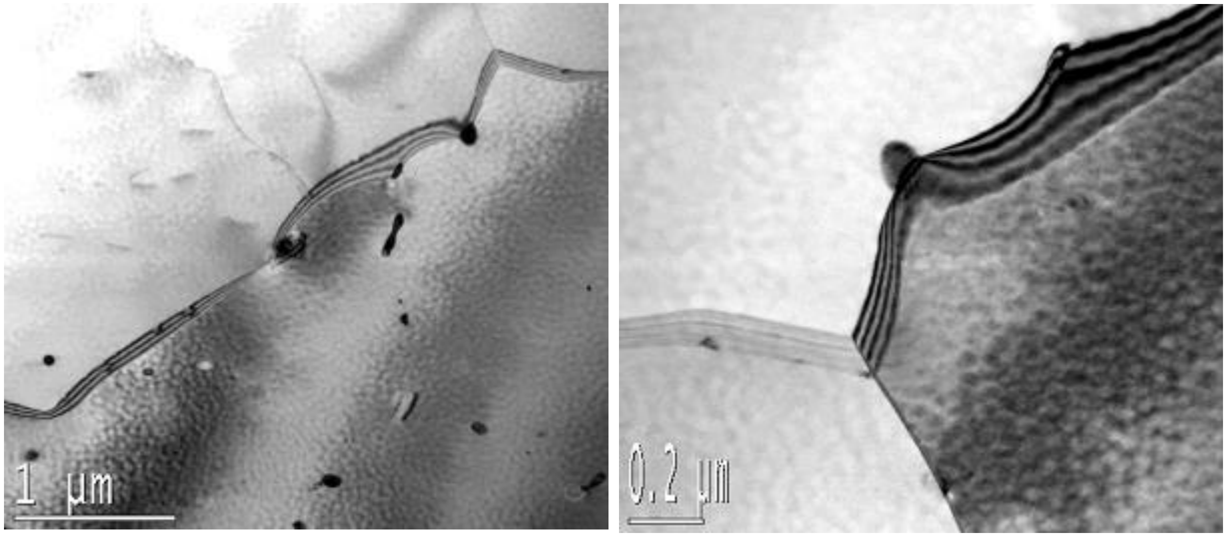

TEM observation of pinning of boundaries by particules

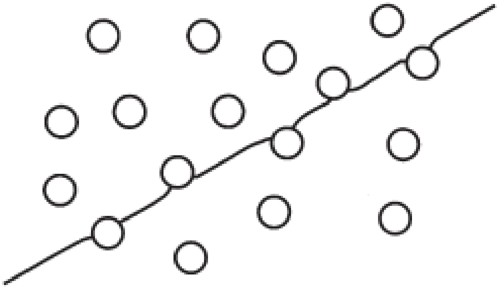

Pinning pressure :

$$P_Z = \frac{3 f \gamma_s}{2r}$$

f = volume fraction
γ_s = grain boundary energy
r = mean particle radius

Recrystallization near porosities in the as-built LPBF state (316L steel): slower cooling rate

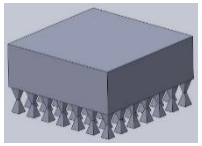

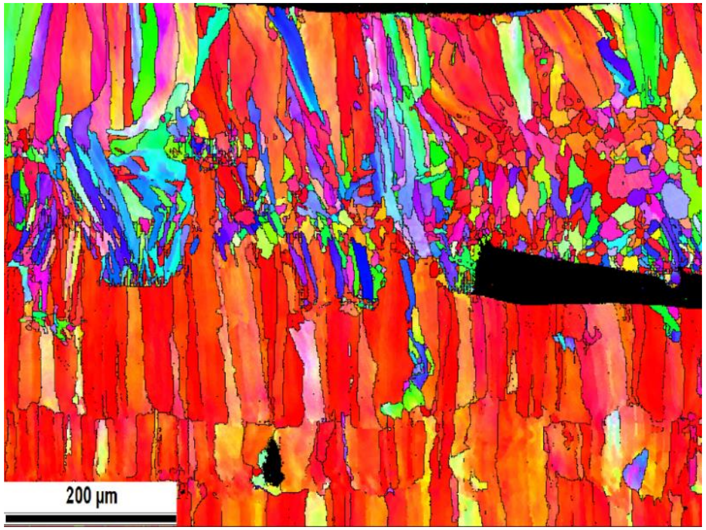

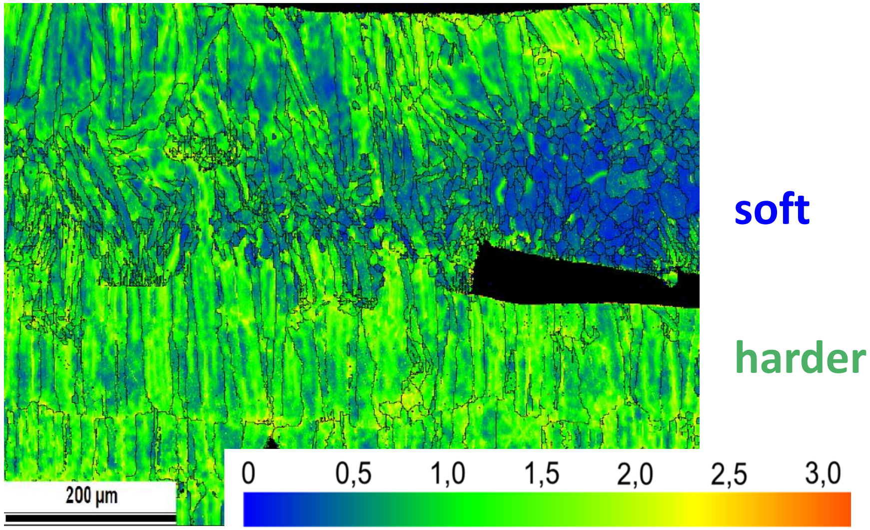

soft

harder

EBSD IPF maps

KAM (misorientation) maps

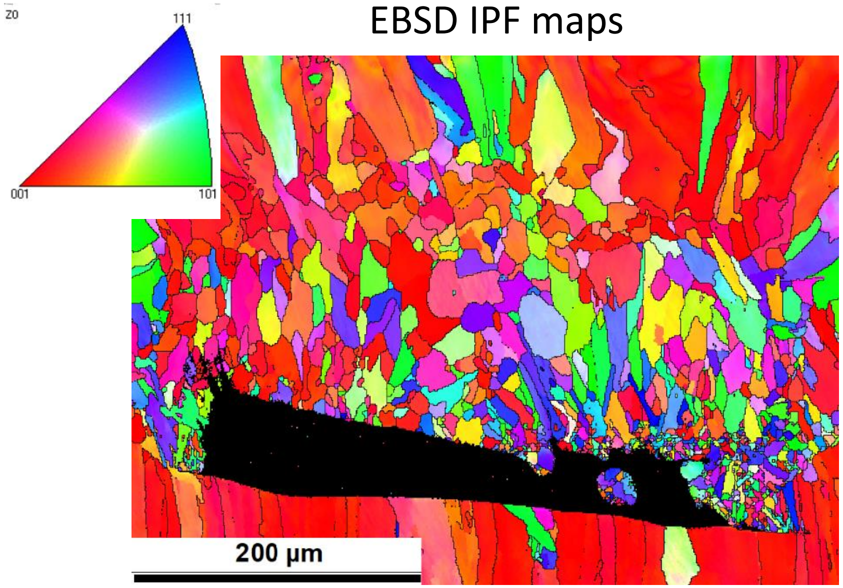

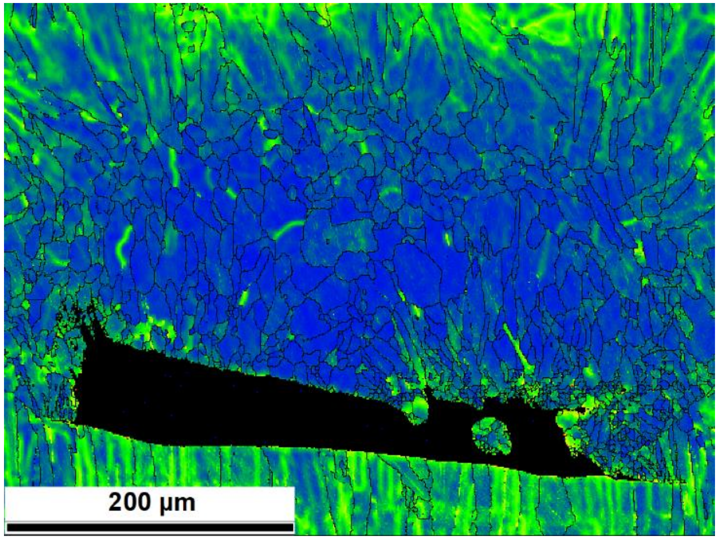

Low stored energy (high normalized enthalpy) : difficult to recrystallize

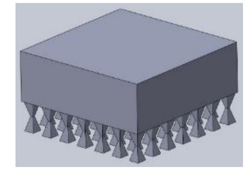

316L steel

<u>3 hours</u>, **3 hours, 1100°C**

As built

BD ↑

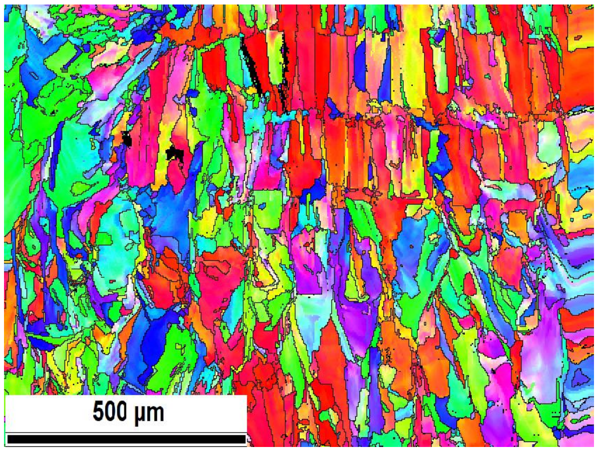

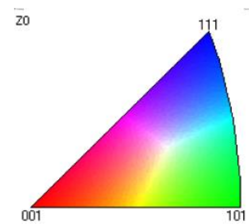

Heat treated

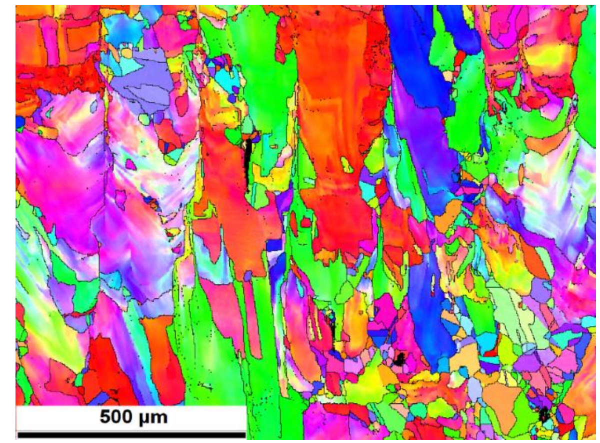

Misorientation map

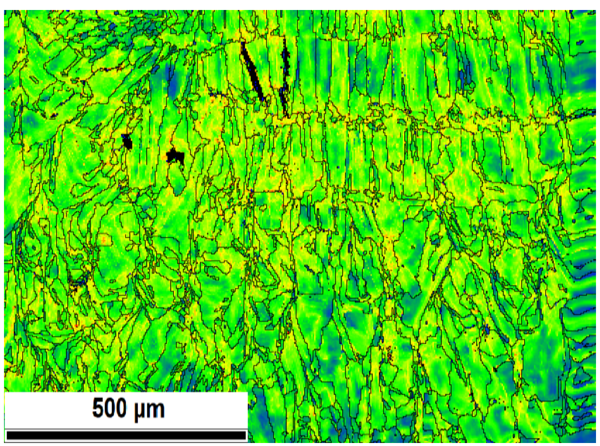

RX fraction ~ 12%

Misorientation map

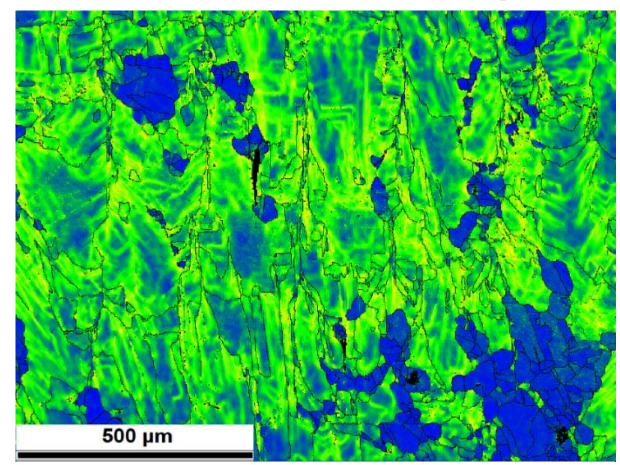

Driving force for recrystallization

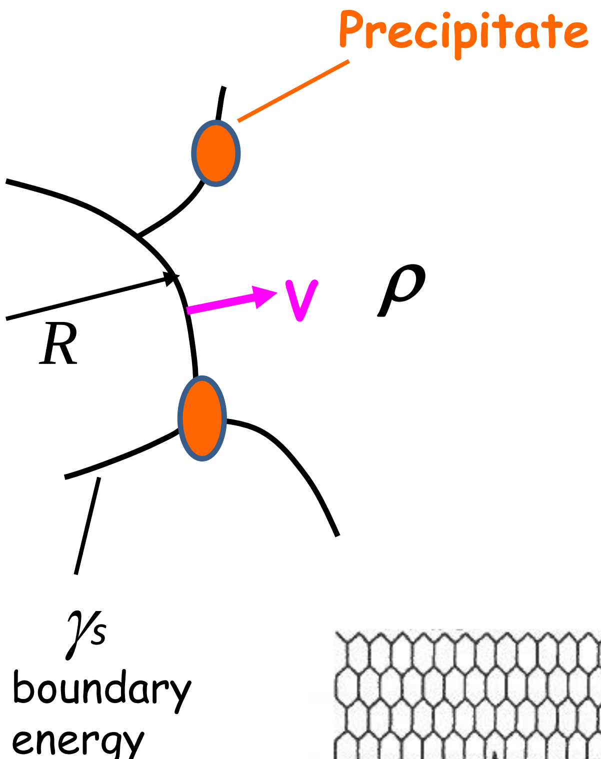

$$V = MP = M\left(E_D + \frac{2\gamma_S}{R} + P_Z\right)$$

Capillary forces, become large if $R < 1\ \mu m$

- $E_D \approx \rho \frac{Gb^2}{2}$ — Energy per unit length of a dislocation
- $M = M_0 \exp\left(-\frac{Q}{RT}\right)$ — Boundary mobility

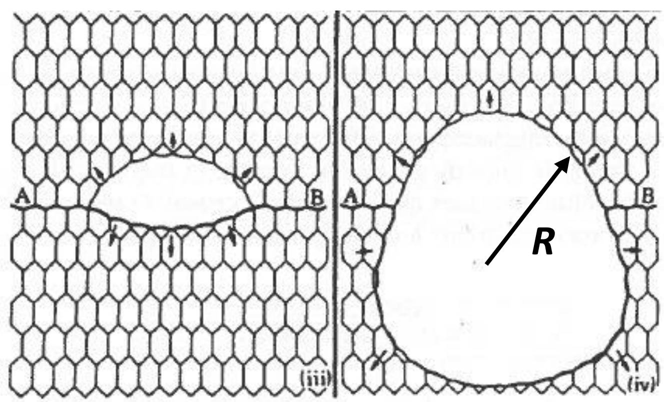

Germination de la recristallisation par coalescence de sous-grains. [Jones et al., 1979]

Nucleation of a dislocation free grain

$$\Delta G = -\frac{4}{3}\pi R^3 E_D + 4\pi R^2 \gamma_s$$

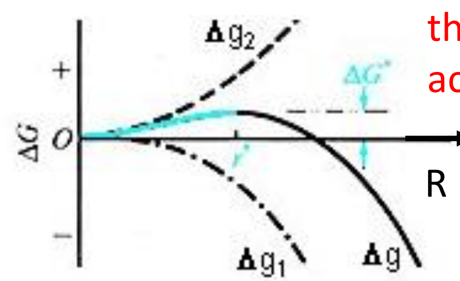

thermally activated

Grain growth

- $\mathbf{V} = M\,P\,\mathbf{n}$ $\qquad$ P = pressure = thermodynamic force

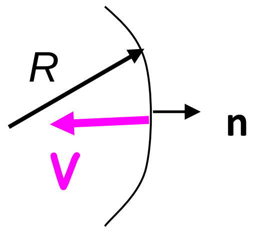

$$P = -\gamma_s \left(\frac{1}{R_1} + \frac{1}{R_2} \right)$$

R_1 and R_2 principal radii of curvature of the boundary

Sphere : $R_1 = R_2 = R$ ➡ $$P = -\frac{2\gamma_s}{R}$$

Thermodynamic force related to grain boundary energy (capillary forces)

→ May be high in AM when dealing with very small grain sizes

- In the presence of **precipitates**

$$V = M\left(\frac{-2\gamma_s}{R} + P_Z \right)$$

$$P_Z = \frac{3f\gamma_s}{2r}$$

Equilibrium grain size :

$$\frac{3f\gamma_s}{2r} = \frac{2\gamma_s}{R} \quad ; \quad R = \frac{4r}{3f}$$

Strength and ductility

$$\tau = \tau_0 + \alpha_1 G b \sqrt{\rho_i} + \alpha_2 \frac{G b}{D} + \alpha_3 \frac{G b}{d}$$

Shear stress for dislocation motion

- ρ_i = dislocation density in the subgrain interior
- D = boundary spacing
- d = precipitates / particles spacing

As always, strength and ductility are opposing properties

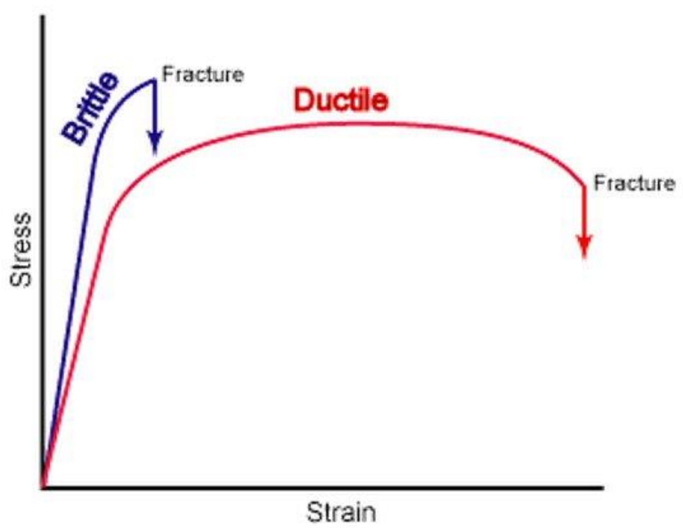

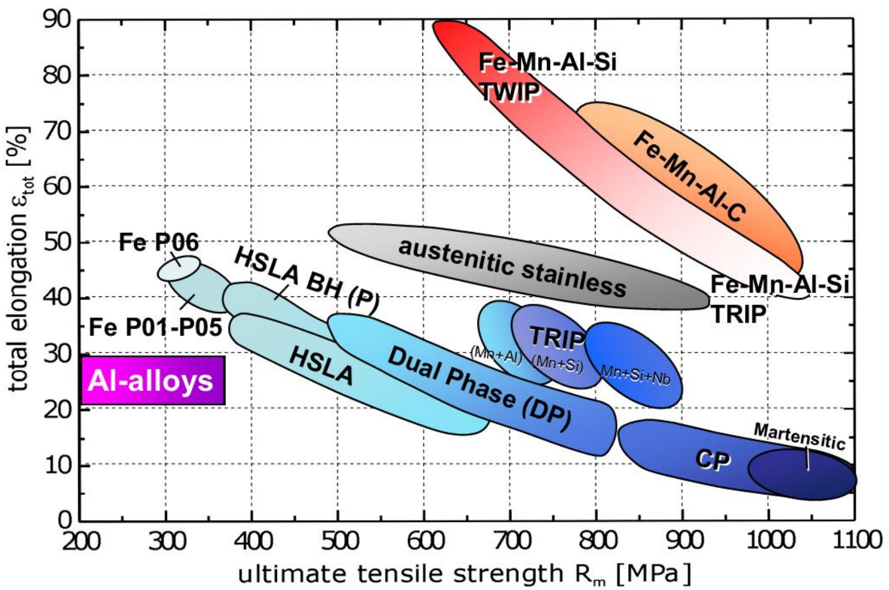

Strength

Ti-6Al-4V AM tensile properties.

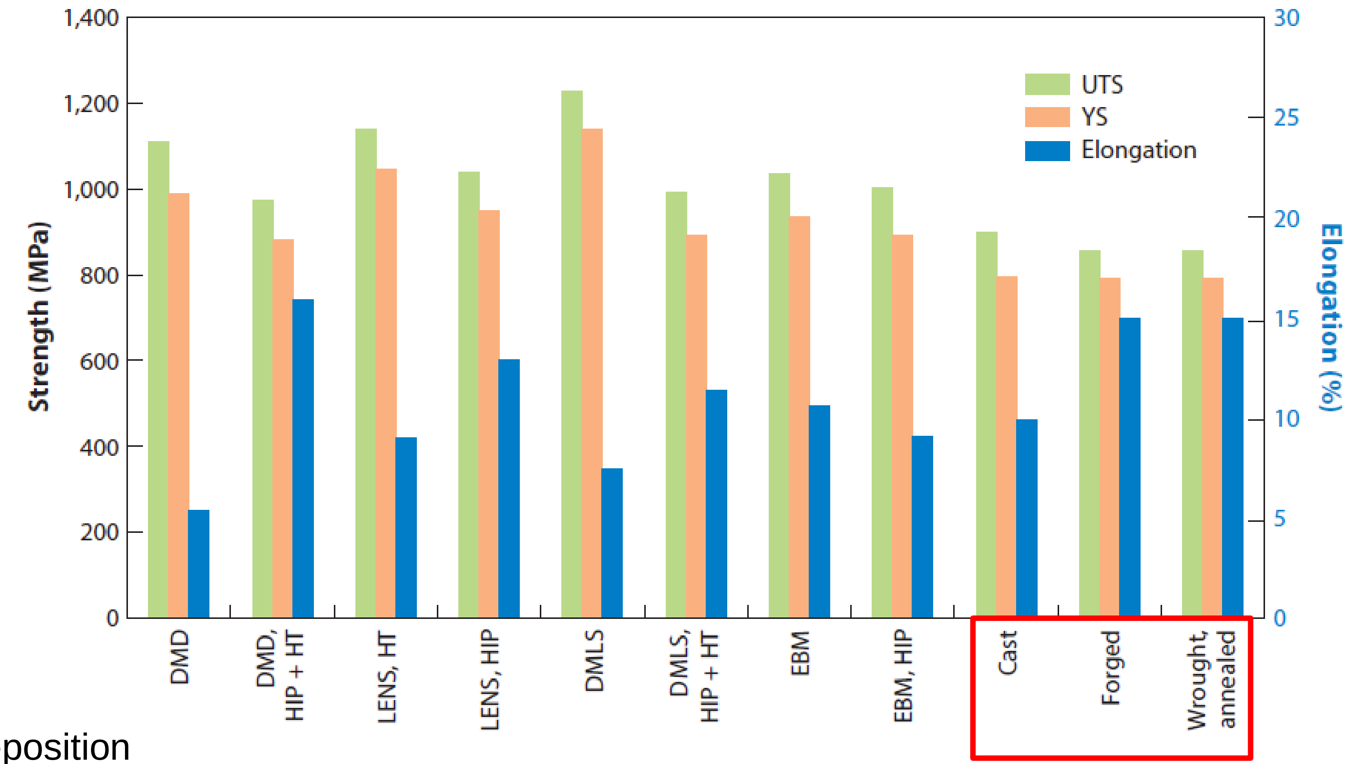

DMD, direct metal deposition
DMLS, direct metal laser sintering;
EBM, electron beam melting;
HT, heat treated;
LENS, laser-engineered net shaping;
UTS, ultimate tensile strength;
YS, yield stress.

Strength usually higher than cast / forged material

J.J. Lewandowski, M. Seifi, Metal Additive Manufacturing: A Review of Mechanical Properties, Annual Review of Materials Research 2016 46:1, 151-186

Toughness

Location-dependent values in an as-built EBM Ti-6Al-4V sample.

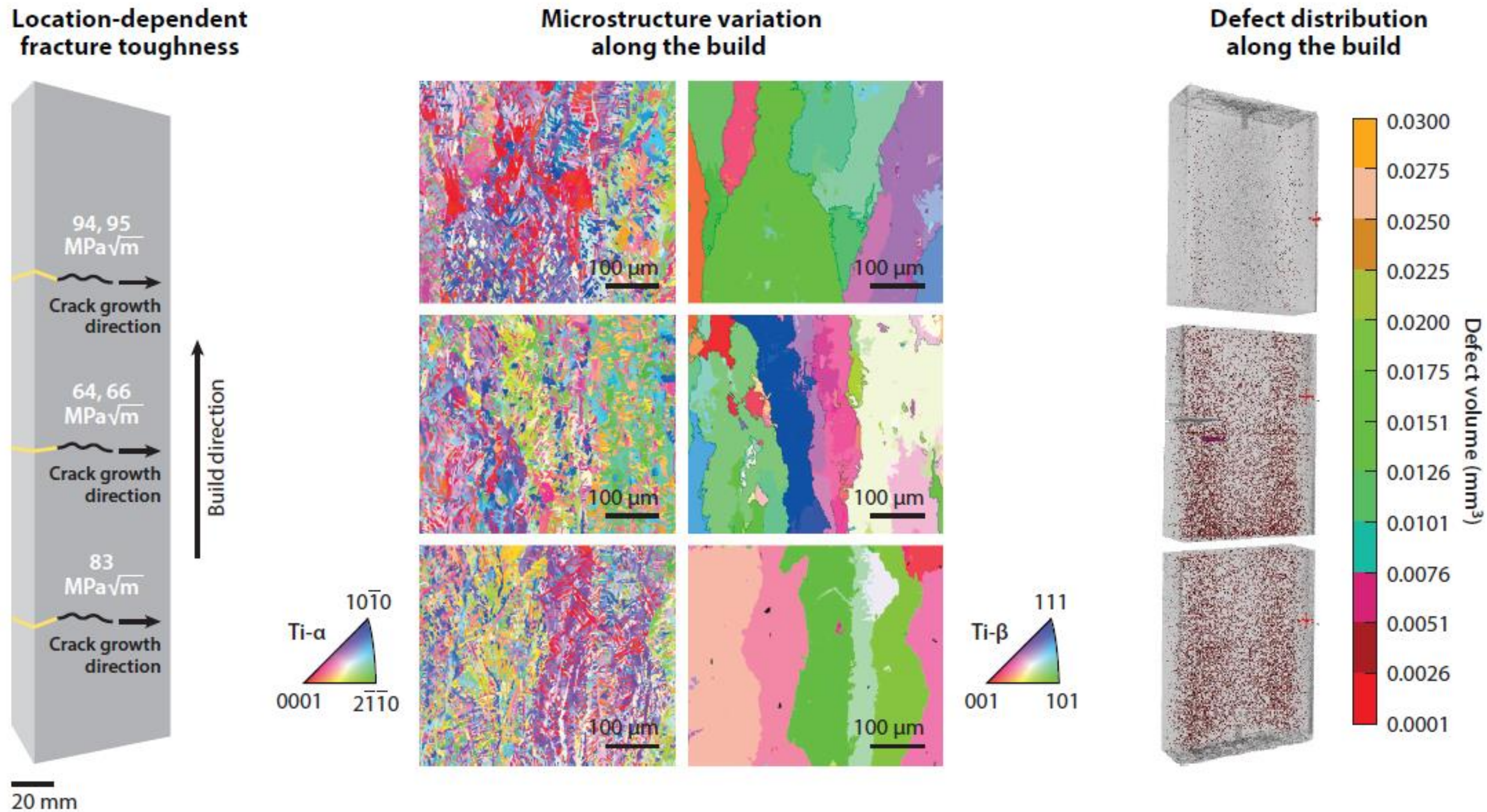

Variations in microstructure (prior β grains and α + β microstructure) and defect density were detected along the same as-built sample

J.J. Lewandowski, M. Seifi, Metal Additive Manufacturing: A Review of Mechanical Properties, Annual Review of Materials Research 2016 46:1, 151-186

Texture and anisotropy

Defining angle θ between tensile direction and rolling direction of the sheet

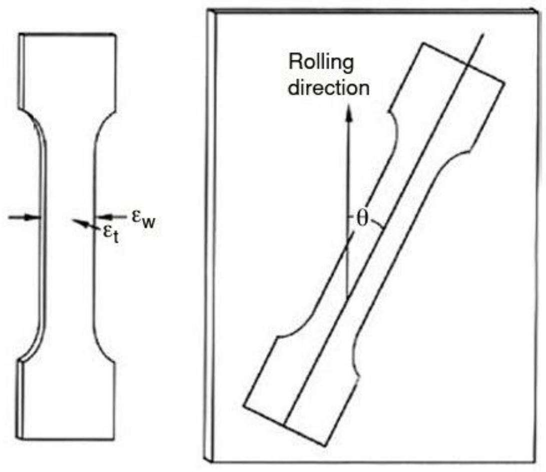

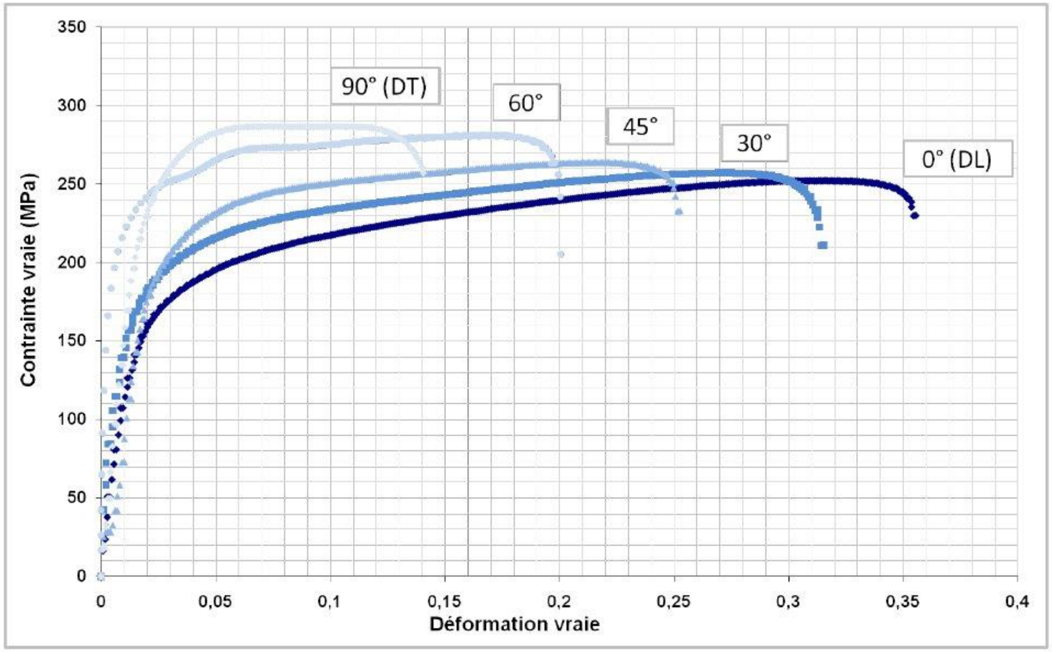

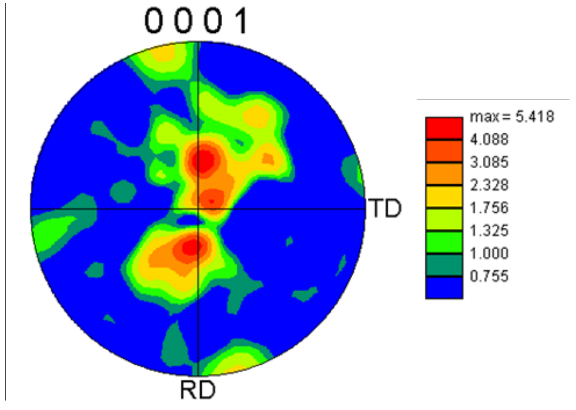

Orientation dependence of mechanical behavior of a Zinc alloy as a function of the angle θ

(Ch. Kerisit, ENSMP).

Texture of an AM part

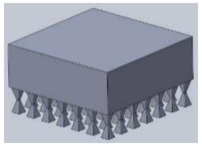

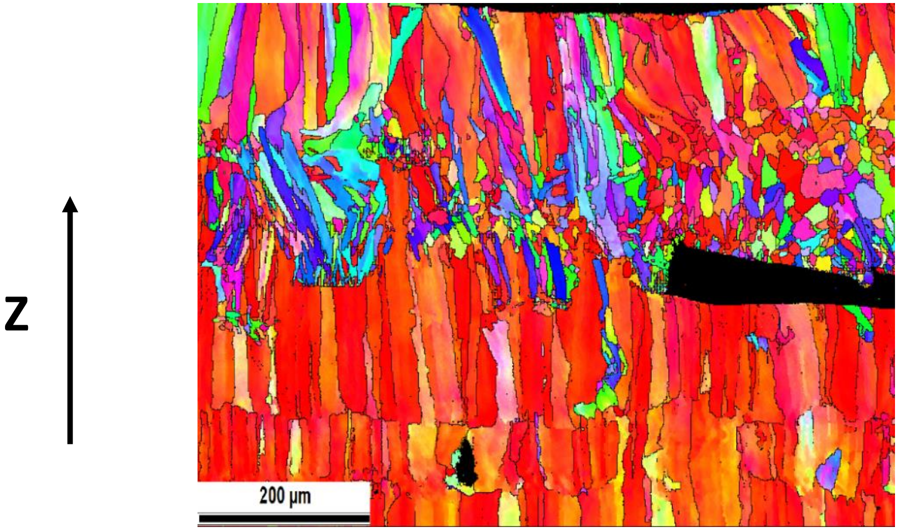

EBSD IPF maps

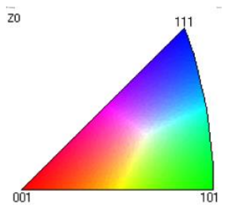

- In cubic materials, <100> is usually // to the build direction Z. This « epitaxial » growth results in a strong crystallographic texture.

- There is also a strong morphological texture due to grains elongated in the Z direction → **directional Hall-Petch effect**

Mechanical Anisotropy of an AM part

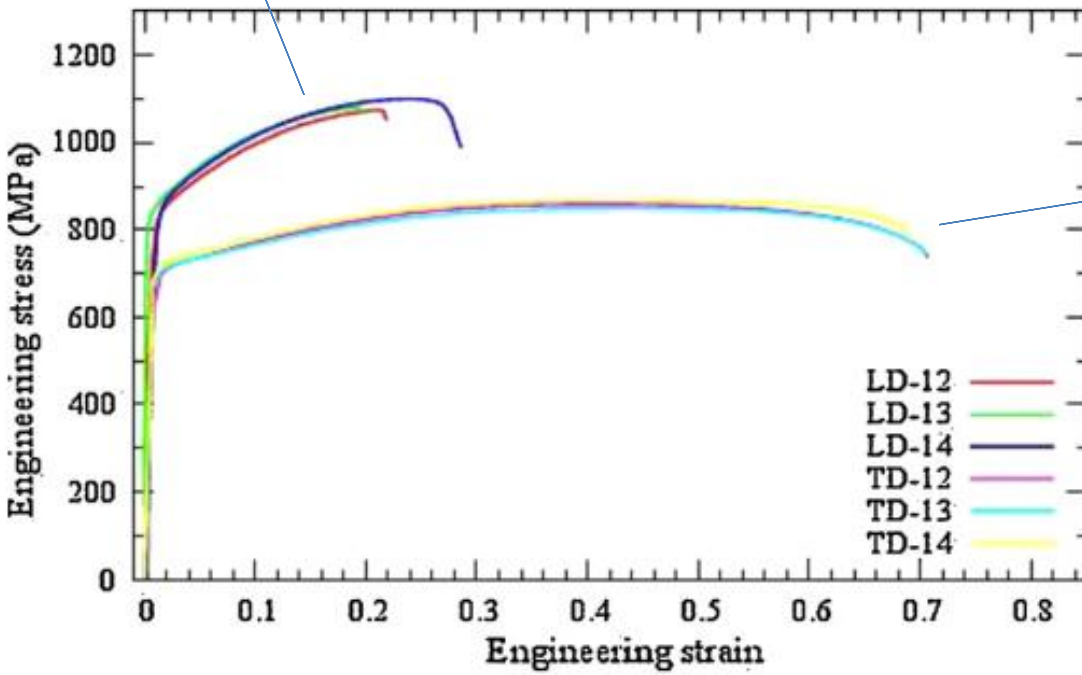

Pulling along Z

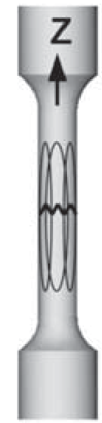

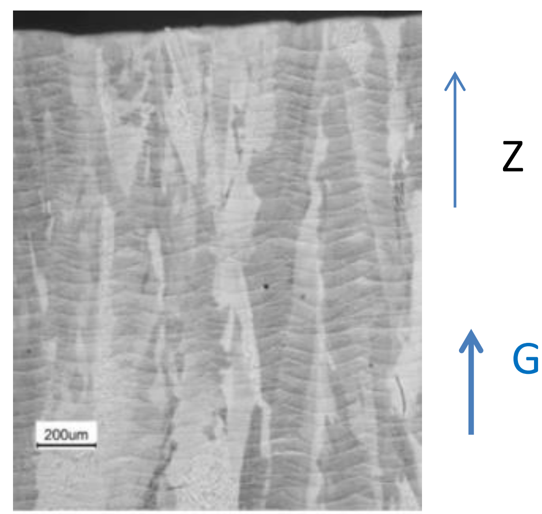

Tensile properties of Nimonic 263
SLM samples

[T. Vilaro et al., Materials Science & Engineering A, 2012]

Mechanical Anisotropy of an AM part

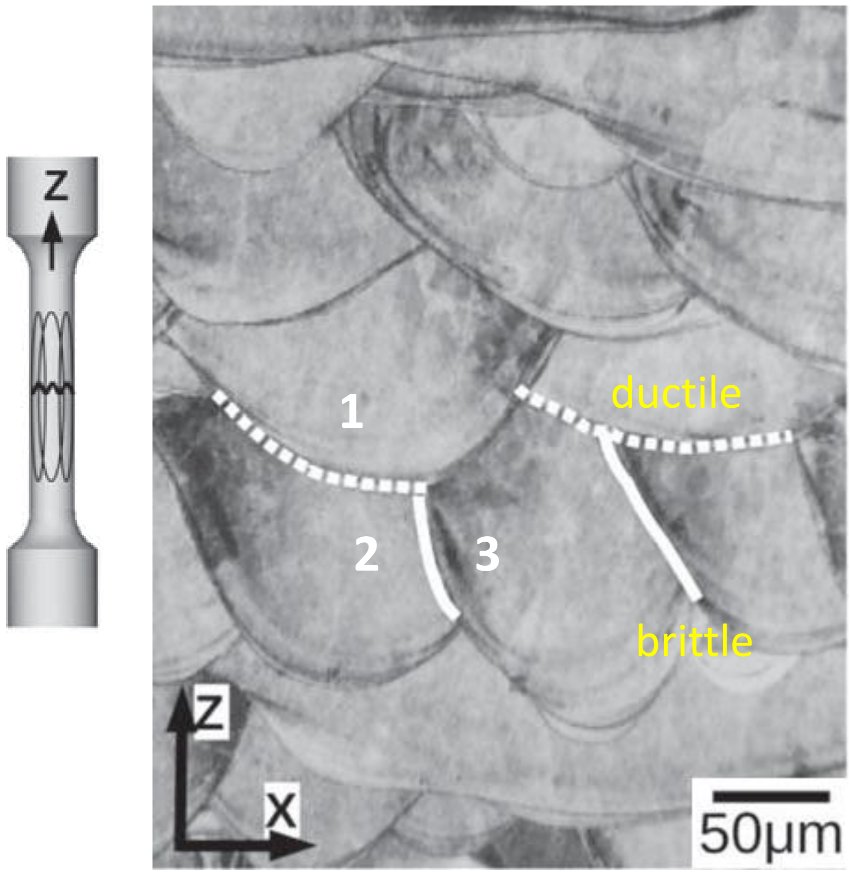

[D. Tomus et al., Materials Science & Engineering A, 2016]

Morphology of the molten pools (Hastelloy-X). Boundaries :

- between two alternating layers (dashed line -- **ductile**)
- between two adjacent molten pools (continuous line -- **brittle**).
  = weak zones, **leading to early failure**

"Disappear" by HIP and/or Heat Treatment

The orientation in space and with respect to the loading direction of these boundaries largely determine the ductility of the as built material.

Mechanical Anisotropy of an AM part

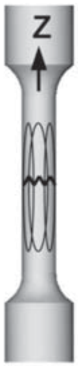

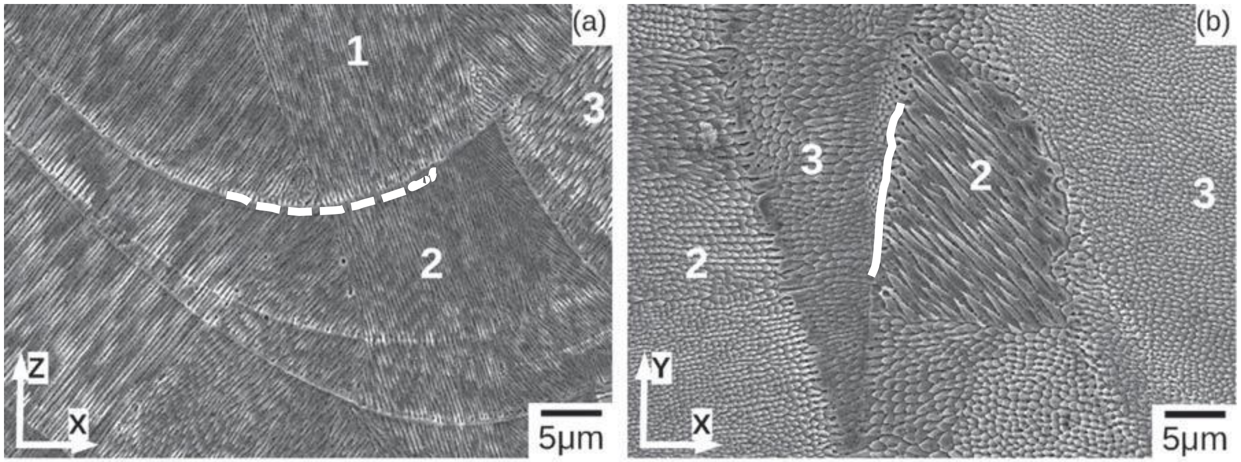

2-3 boundaries more prone to failure

[D. Tomus et al., Materials Science & Engineering A, 2016]

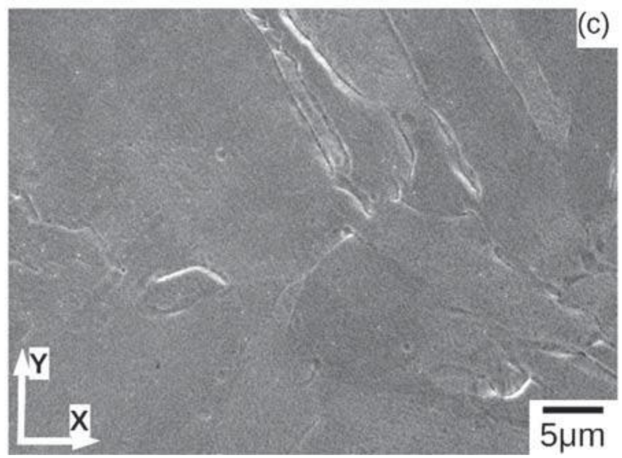

Heat treated sample: Dissolution of dendrites

Dendrites tend to extend their orientation between alternating layers (1-2) whereas they change the direction between adjacent layers (2-3)

Cyclic loading and low cycle fatigue

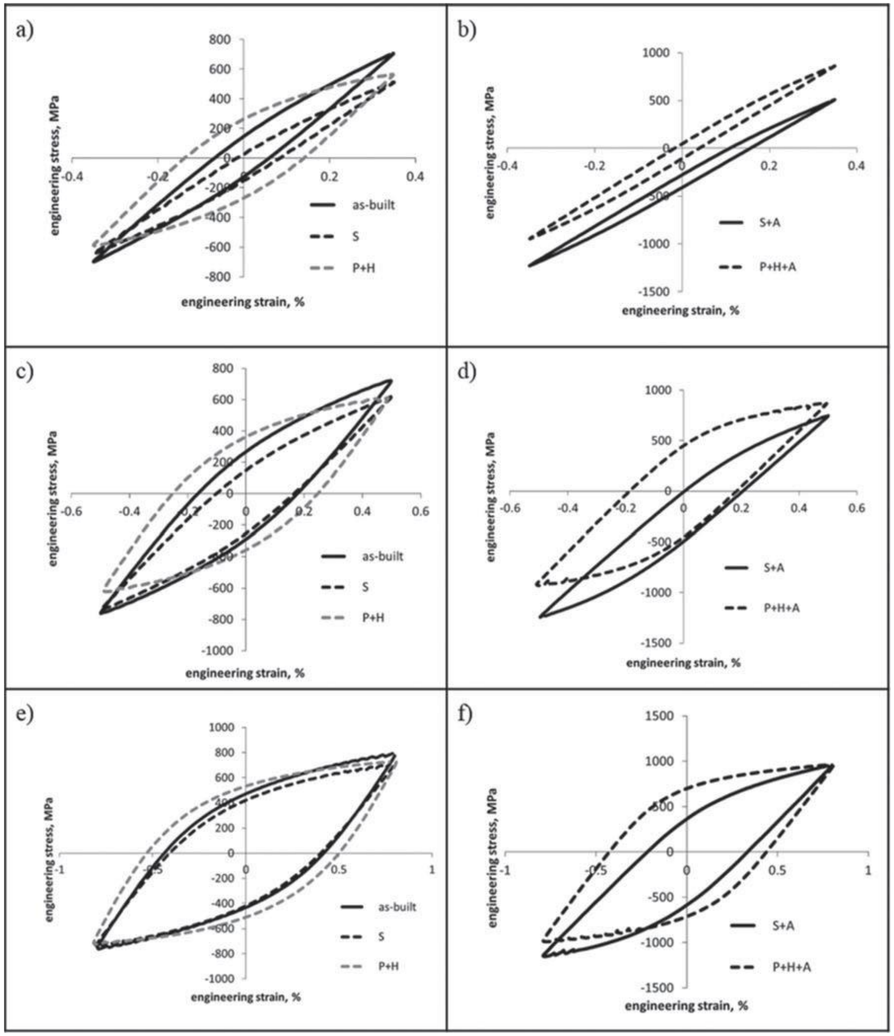

[M.E. Aydinöz et al., Materials Science & Engineering A 2016]

- **Inconel 718 : Different behaviors** for as-built, solution annealed, and HIPed samples

- **Main influencing factors** :
  - dislocation structure – cell structure (as-built, solution annealed)
  - grain structure – large grains in HIPed grains due to recrystallization & grain growth
  - residual stresses, may evolve with cycling

Low Cycle Fatigue, Half-life cycle

High cycle fatigue

- Any porosity left may contribute to a reduced fatigue life
- Roughness is detrimental

→ Both induce stress concentration

Porosities

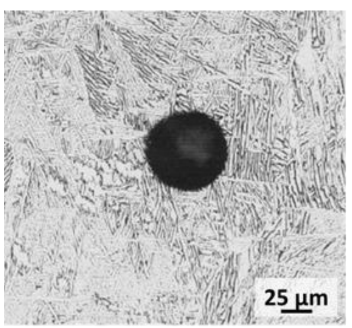

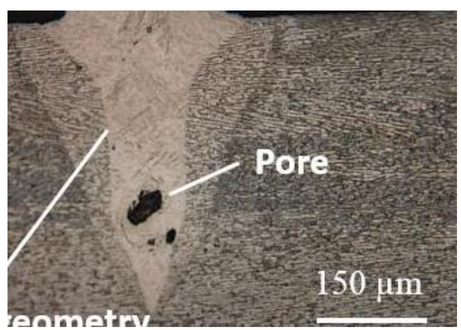

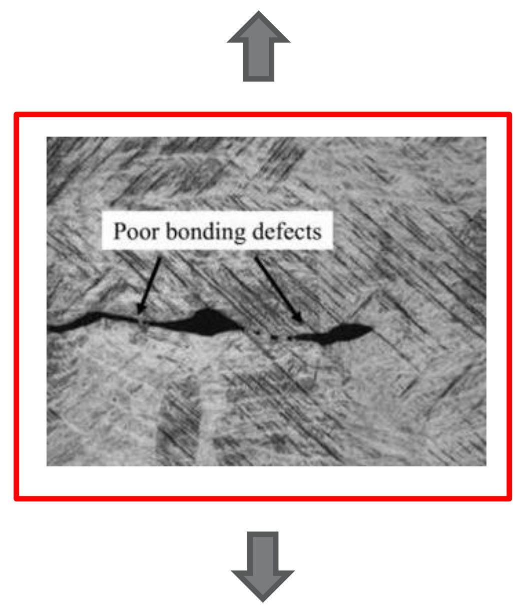

Which one is the most detrimental ?

High cycle fatigue

Elliptical porosity

Griffith theory

$$\sigma_y^{local} = \sigma^{applied}\left(1+2\sqrt{\frac{a}{r}}\right)$$

$$= \sigma^{applied}\left(1+2\frac{a}{h}\right)$$

$$= K_t\,\sigma^{applied}$$

K_t = Stress concentration factor

Radius of curvature

$$r = \frac{h^2}{a}$$

$\sigma^{applied}$

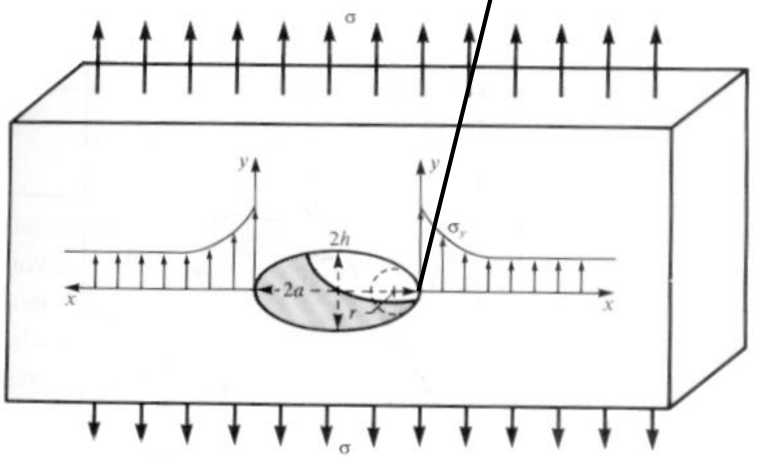

$\sigma^{applied}$

The smaller the radius of curvature, the larger the local stresses

→ **The shape of porosities matters**

→ Lack of fusion defects

High cycle fatigue

Roughness

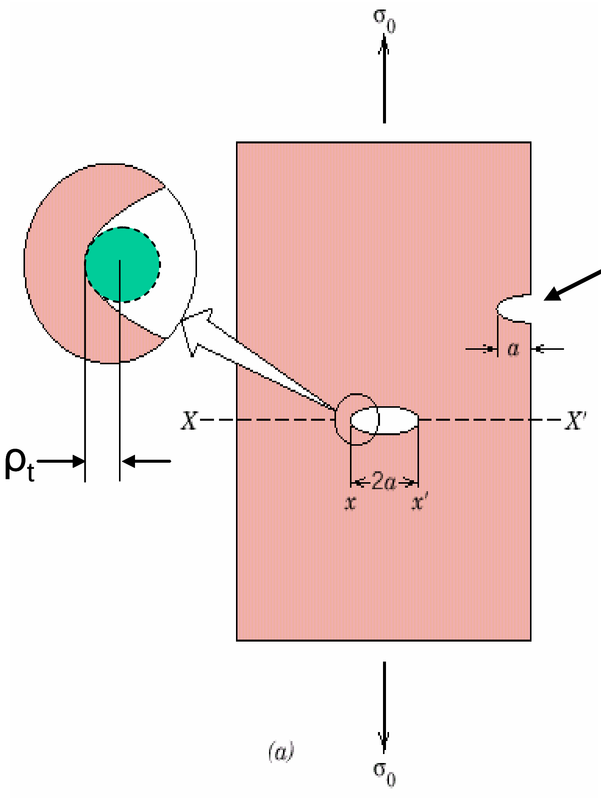

Stress concentration at the surface : notch, or **surface roughness**

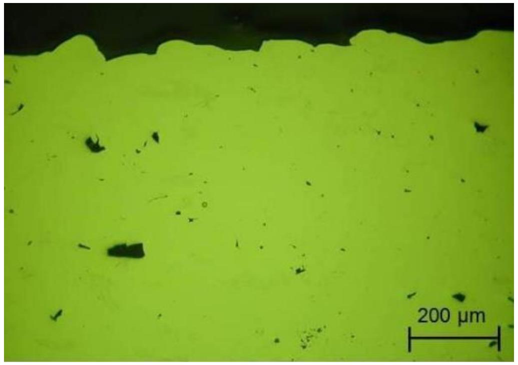

High cycle fatigue

Stress amplitude
(MPa)

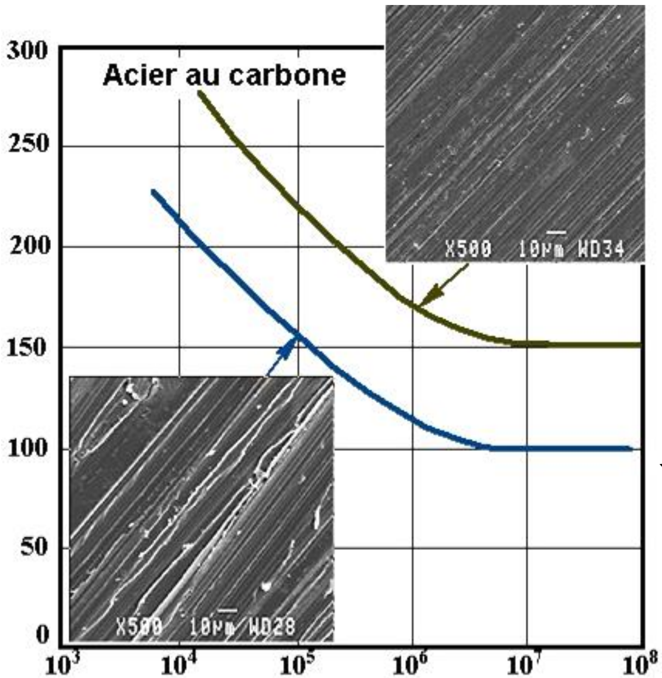

Number of cycles to failure

Increasing the strength of the material = increasing the fatigue life.

Fatigue strength :
35% to 65% of the tensile strength

Competition between higher strength of AM parts, and impact of defects / roughness

Damage mechanics : the size of porosities matters

S_D is the damaged part of the surface (porosity), designated as dAc

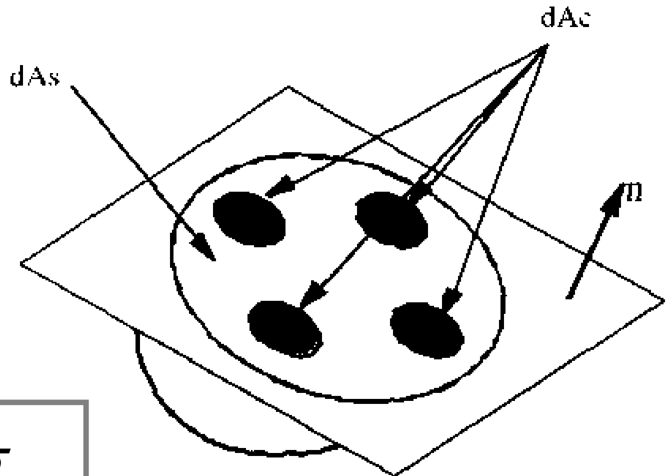

$$D = \frac{S_D}{S}$$

damage

$$0 \leq D \leq 1$$

F / S

$$\tilde{\sigma} = \frac{\sigma}{(1-D)}$$

• **Effective stress** : stress computed from the real area bearing the load

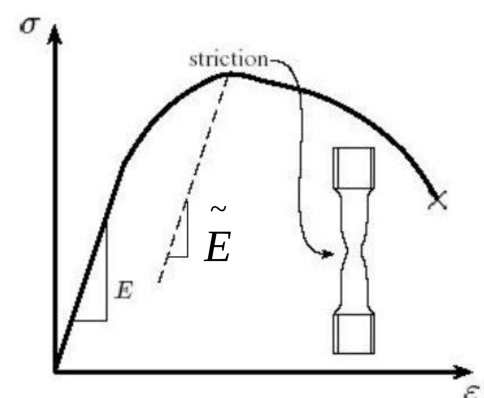

Measuring *D*

• **Influence of *D***:

σ_y and E → *(1-D)

- Yield stress : $\tilde{\sigma} = \sigma_y$ ⇨ $\sigma = \sigma_y(1-D)$
- Effective Young's modulus

$$\tilde{\sigma} = E\varepsilon \Rightarrow \sigma = E(1-D)\varepsilon = \tilde{E}\varepsilon \Rightarrow \tilde{E} = E(1-D)$$

Influence of porosity orientation on ductility

Orientation of porosities

X-Ray tomography

Stress-strain curve

longitudinal

radial

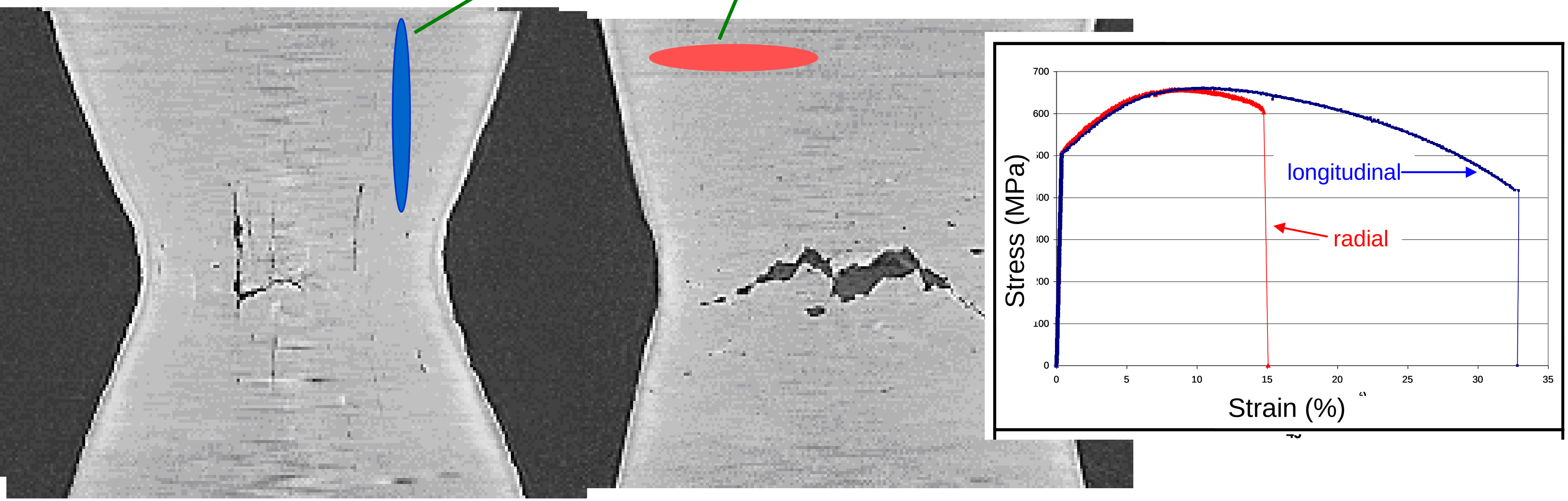

(P.O. Bouchard et al., On the influence of particle distribution and reverse loading on damage mechanisms of ductile steels, *Materials Science and Engineering A*, *2008, 496, 1-2, pp. 223-233*)

High cycle fatigue

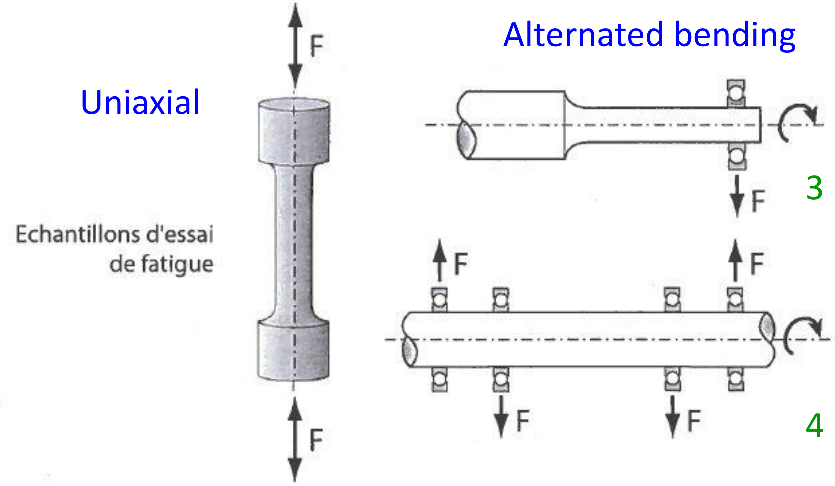

Uniaxial

Alternated bending

3 points

4 points

Residual stresses

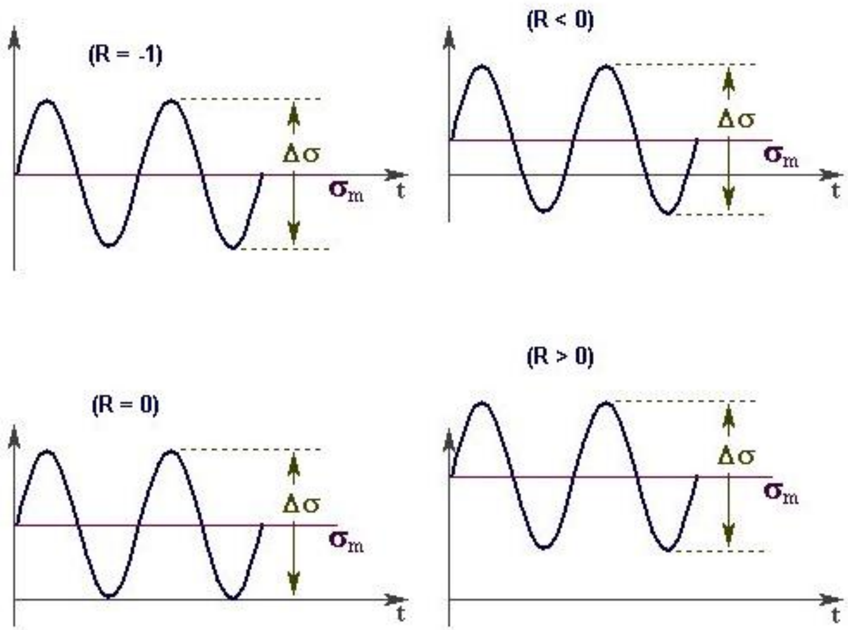

Tensile residual stresses

A major problem in AM

$$R = \frac{\sigma_{\min}}{\sigma_{\max}}$$

Stress ratio

High cycle fatigue

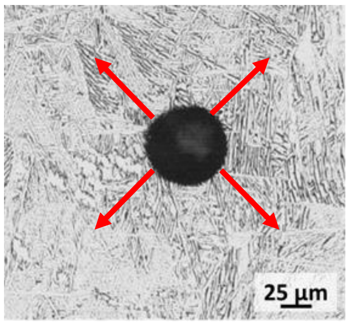

Residual stresses

Porosity growth ~ $\exp(\eta) \;;\; \eta = \dfrac{tr(\sigma)}{\sigma_{eq}}$ Stress triaxiality

Influence of residual stresses on Wöhler's curve

Stress amplitude (MPa)

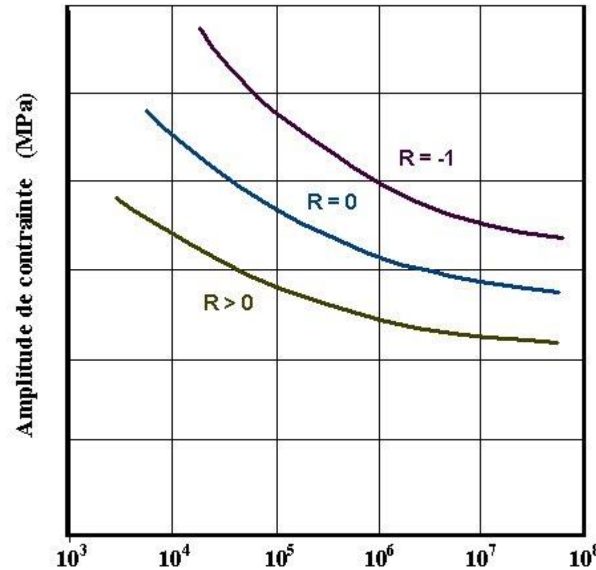

η

Number of cycles to failure

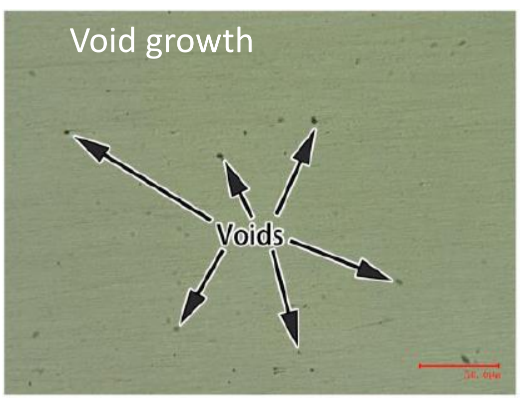

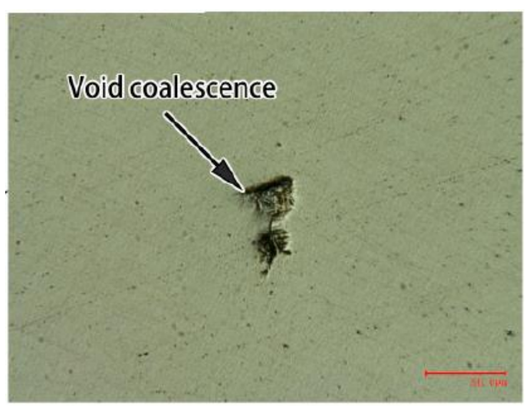

Evolution with number of cycles

Ti-64 defect dominated fatigue behavior

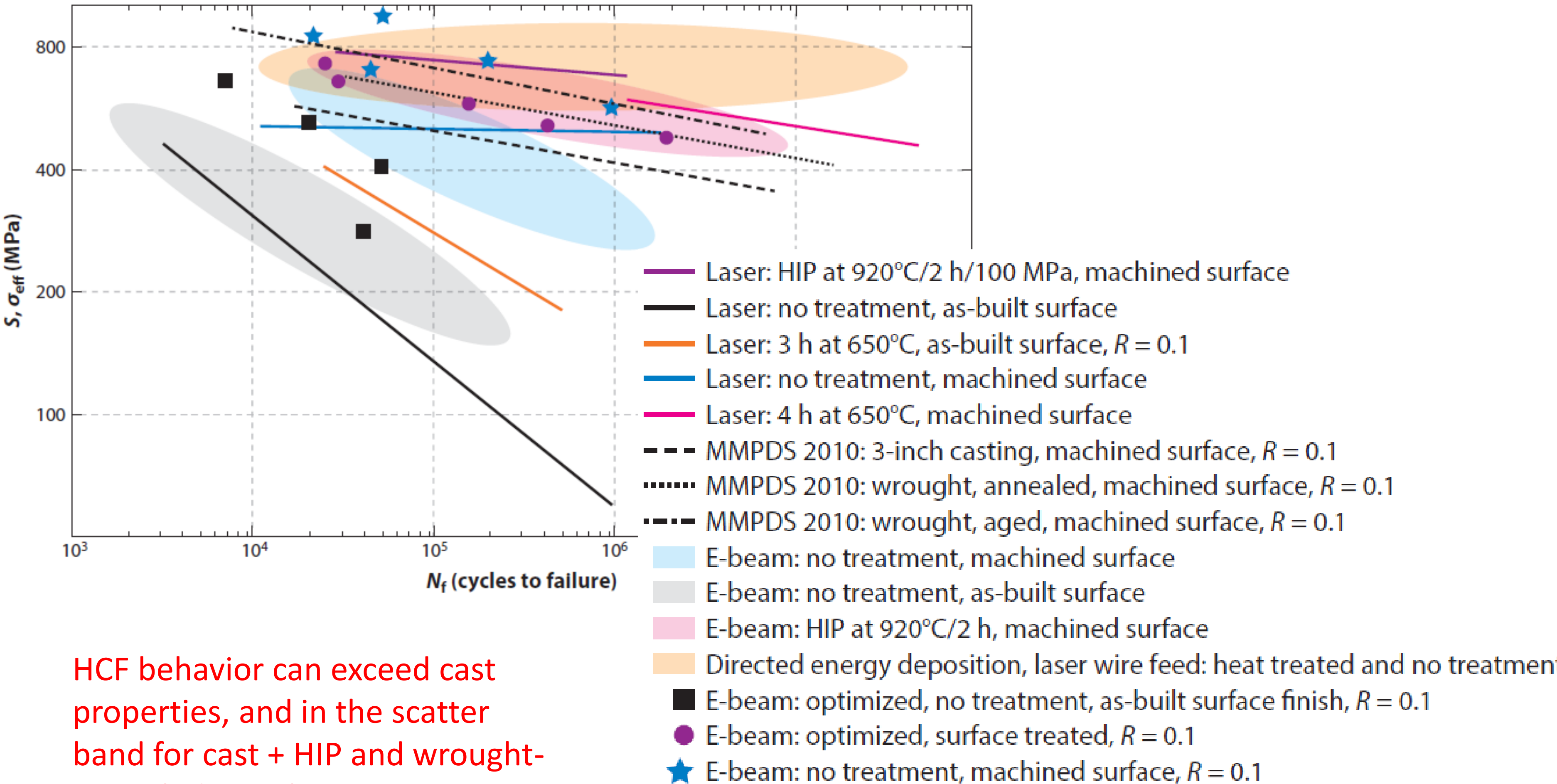

HCF behavior can exceed cast properties, and in the scatter band for cast + HIP and wrought-annealed Ti-6Al-4V

J.J. Lewandowski, M. Seifi, Metal Additive Manufacturing: A Review of Mechanical Properties, Annual Review of Materials Research 2016 46:1, 151-186